

**EDITORIAL COPY**

UNIVERSITY OF MINNESOTA  
ST. ANTHONY FALLS HYDRAULIC LABORATORY  
LORENZ G. STRAUB, Director

Technical Paper No. 20, Series B

# Hydraulics of Closed Conduit Spillways

## Part X. The Hood Inlet

by

Fred W. Blaisdell and Charles A. Donnelly  
Hydraulic Engineers, USDA, ARS



April 1958

Study conducted by

UNITED STATES DEPARTMENT OF AGRICULTURE  
AGRICULTURAL RESEARCH SERVICE  
SOIL AND WATER CONSERVATION RESEARCH DIVISION

in cooperation with the

Minnesota Agricultural Experiment Station  
and the  
St. Anthony Falls Hydraulic Laboratory

Minneapolis, Minnesota

UNIVERSITY OF MINNESOTA  
ST. ANTHONY FALLS HYDRAULIC LABORATORY  
LORENZ G. STRAUB, Director

Technical Paper No. 20, Series B

# Hydraulics of Closed Conduit Spillways

## Part X. The Hood Inlet

by

Fred W. Blaisdell and Charles A. Donnelly  
Hydraulic Engineers, USDA, ARS



April 1958

Study conducted by

UNITED STATES DEPARTMENT OF AGRICULTURE  
AGRICULTURAL RESEARCH SERVICE  
SOIL AND WATER CONSERVATION RESEARCH DIVISION

in cooperation with the

Minnesota Agricultural Experiment Station  
and the  
St. Anthony Falls Hydraulic Laboratory

Minneapolis, Minnesota

## A B S T R A C T

Comprehensive experiments on the hood inlet for closed conduit spillways are reported. The capacity and performance of the spillway for variations of the hood inlet length, the conduit slope, the wall thickness and the approach conditions are described. The great effect of vortices on the spillway capacity is shown and anti-vortex devices are developed. Scour in the vicinity of the hood inlet is determined for various sizes of stone and equations for the scour hole dimensions are presented. A few special inlets were tested, the effect of rounding the entering edge being the principal variation.

# C O N T E N T S

	Page
Abstract . . . . .	iii
List of Figures . . . . .	vi
List of Tables . . . . .	vii
FORWARD . . . . .	1
PART X. THE HOOD INLET . . . . .	1
INTRODUCTION . . . . .	1
PREVIOUS WORK . . . . .	1
EXPERIMENTAL PROGRAM . . . . .	2
Hood Length . . . . .	3
Conduit Slope . . . . .	3
Wall Thickness . . . . .	3
Entrance Shape . . . . .	3
Anti-Vortex Device . . . . .	3
Approach Conditions . . . . .	3
Scour . . . . .	3
TEST APPARATUS . . . . .	3
TEST PROCEDURE . . . . .	7
ANALYTICAL METHODS . . . . .	9
RESULTS OF TESTS . . . . .	10
Spillway Performance . . . . .	10
Optimum Hood Length . . . . .	10
Conduit Slope . . . . .	15
Vortex Inhibitor . . . . .	17
Conduit Wall Thickness . . . . .	19
Special Inlets . . . . .	20
Sliced Inlet . . . . .	20
Well-Rounded Re-entrant Inlet . . . . .	20
Well-Rounded Re-entrant Hood Inlet . . . . .	21
Approach Conditions . . . . .	22
Scour at Hood Inlet . . . . .	22
Spillway Capacity . . . . .	27
Capacity as a Weir . . . . .	27
Hood Length . . . . .	27
Conduit Slope . . . . .	27
Conduit Wall Thickness . . . . .	28
Approach Conditions . . . . .	28
Special Inlets . . . . .	28
Head-Discharge Equations . . . . .	30
Comparison with Mavis' Curve . . . . .	32
Entrance Loss for Full Conduit Flow . . . . .	32
Conduit Slope . . . . .	32
Hood Length . . . . .	32
Conduit Wall Thickness . . . . .	32
Anti-Vortex Device . . . . .	33
Approach Conditions . . . . .	34
Special Inlets . . . . .	34

	Page
Capacity as an Orifice .....	35
Pressures .....	36
Hydraulic Grade Line .....	36
CONCLUSIONS AND RECOMMENDATIONS .....	41
ACKNOWLEDGEMENTS .....	41

L I S T O F F I G U R E S

Figure		Page
X-1	Hood Inlet and Anti-Vortex Device . . . . .	2
X-2	Definition of Terms . . . . .	2
X-3	Perspective Sketch of Test Apparatus . . . . .	5
X-4	Water Level Recorder Chart, Series 85 . . . . .	8
X-5	Manometer Board, Series 85, Run 14 . . . . .	9
X-6	Average Priming Head as a Function of the Hood Length . . . . .	11
X-7	Appearance of the Hood Inlet as the Headpool Level Rises and the Inlet Primes . . . . .	12
X-8	Some Conditions of Conduit Flow . . . . .	13
X-9	Effect of Hood Length on Flow at the Inlet for $\frac{H}{D} = 1.0$ . . . . .	14
X-10	Effect of Conduit Slope on the Head-Discharge Relationship . . . . .	15
X-11	Effect of the Presence or Absence of an Anti-Vortex Device on the Spillway Capacity . . . . .	16
X-12	Anti-Vortex Devices . . . . .	18
X-13	Comparison of Head-Discharge Curves for Different Anti-Vortex De- vices . . . . .	19
X-14	Proportions of Special Inlets . . . . .	20
X-15	Head-Discharge Curves for Special Inlets . . . . .	21
X-16	Size Distribution of Sands Used for Scour Tests . . . . .	23
X-17	Scour Hole Radius . . . . .	25
X-18	Grain Size for Imminent Movement . . . . .	25
X-19	Scour Hole Depth . . . . .	25
X-20	Effect of Hood Length on Weir Flow Head-Discharge Relationship . .	26
X-21	Effect of Conduit Slope on Weir Flow Head-Discharge Relationship .	27
X-22	Effect of Conduit Wall Thickness on Weir Flow Head-Discharge Re- lationship . . . . .	28
X-23	Effect of Approach on Weir Flow Head-Discharge Relationship . . . .	29
X-24	Head-Discharge Curves for Weir Flow for Well-Rounded Re-entrant, Well-Rounded Re-entrant Hood, and Sliced Inlets . . . . .	29
X-25	Comparison of Hood Inlet Weir Flow Head-Discharge Equations with Mavis' Curve . . . . .	31
X-26	Effect of Hood Length on Entrance Loss Coefficient . . . . .	32
X-27	Effect of Conduit Wall Thickness on Entrance Loss Coefficient . . . .	33
X-28	Head-Discharge Curves for Short Hood Lengths Where the Entrance Orifice May Control . . . . .	35
X-29	Discharge Coefficient for Orifice Control . . . . .	37
X-30	Influence of Hood Length on Pressures in Conduit 0.5D Downstream from the Entrance . . . . .	38
X-31	Effect of Wall Thickness on Pressure . . . . .	39
X-32	Position of the Hydraulic Grade Line at the Conduit Exit . . . . .	40

L I S T O F T A B L E S

Table		Page
X-1	Summary of Tests . . . . .	4
X-2	Prime Heads for Different Hood Lengths and Conduit Slopes . . . . .	10
X-3	Sizes of Bed Material Used for Scour Tests . . . . .	22
X-4	Scour Hole Dimensions . . . . .	24
X-5	Values of $\frac{a}{A} \sqrt{\frac{H}{D}}$ . . . . .	31
X-6	Effect of Anti-Vortex Device on Entrance Loss Coefficient and Pressure . . . . .	32
X-7	Effect of Approach on Entrance Loss Coefficient and Pressure . . . . .	34
X-8	Entrance Loss Coefficients and Pressures for Special Inlets . . . . .	34

# HYDRAULICS OF CLOSED CONDUIT SPILLWAYS

## FORWARD

This technical paper is one of a series on the hydraulics of closed conduit spillways. Part I, giving the theory, symbols and bibliography, appeared originally in 1952 as Technical Paper No. 12-B. It was revised in 1958. Parts II to VI, describing the hydraulic performance and presenting discharge coefficients for five forms of the closed conduit spillway, and Part VII discussing vortices and their effect on the spillway capacity appeared as Technical Paper No. 18-B. Parts VIII and IX, reporting tests on models of specific field structures and on field structures themselves, appeared as Technical Paper No. 19-B. The present paper, Part X of the series, describes the development of the hood inlet first reported by Karr and Clayton [I-28].

## Part X

### The Hood Inlet\*

## INTRODUCTION

Renewed interest in the hydraulic performance of culverts is evidenced by the number of studies reported since 1950. One reason is because the hydraulics of culverts and other types of closed conduit spillways is not as simple as was once thought. Another reason is because large numbers of these structures are being built each year and small savings or improvements in each structure result in large totals.

Many of the studies have been on the inlet and its effect on the overall performance of the spillway. Square-edged entrances and re-entrant, sharp-edged entrances have been found to have poor hydraulic characteristics for many purposes. Well-rounded entrances, flared entrances and drop inlets have been developed to overcome some of the objections to the poorer inlets. Nevertheless, objections still persist in some cases because of the careful workmanship required and the high cost of the inlets. Search for a simple inlet having good hydraulic performance has continued. The hood inlet, discovered and briefly tested by Karr and Clayton [I-28] at Oregon State College, appeared to be a simple, economical, and easily installed inlet that would be particularly useful to the Soil Conservation Service in connection with their work with soil conservation districts where the structures are installed by the landowner. The agricultural conservation, flood prevention, and watershed protection programs of the U. S. Department of Agriculture also would have use for this type of inlet. Accordingly, at the request of the Soil Conservation Service a thorough study of the hood inlet was initiated by the Agricultural Research Service at the St. Anthony Falls Hydraulic Laboratory. Considerable savings appeared possible as a result of the use of this inlet as a spillway inlet for farm ponds, irrigation ponds, flood detention and watershed protection reservoirs, and other soil and water conservation structures. The number of ponds and reservoirs built in 1954, the most recent year for which figures are available, was 160,976, and the simple spillway inlet would have been adaptable to many of them.

As shown in Figs. X-1 and X-2, the hood inlet is formed by cutting a pipe at an angle and laying the pipe so the longer side is at the crown. This forms a hood over the pipe entrance. The name was selected by Agricultural Research Service and Soil Conservation Service conferees as being descriptive of the inlet.

## PREVIOUS WORK

Background for the hood inlet study is derived from a number of sources. The current work can be considered as the development of the idea originated by Karr and Clayton [I-28] at Oregon State College. Their work was carried far enough to indicate the potentialities of the hood inlet and to show the desirability of giving it detailed study.

The work of Beasley and Meyer [I-4] at the University of Missouri was published during

---

\*Agricultural Research Service Report No. 41-505-75.



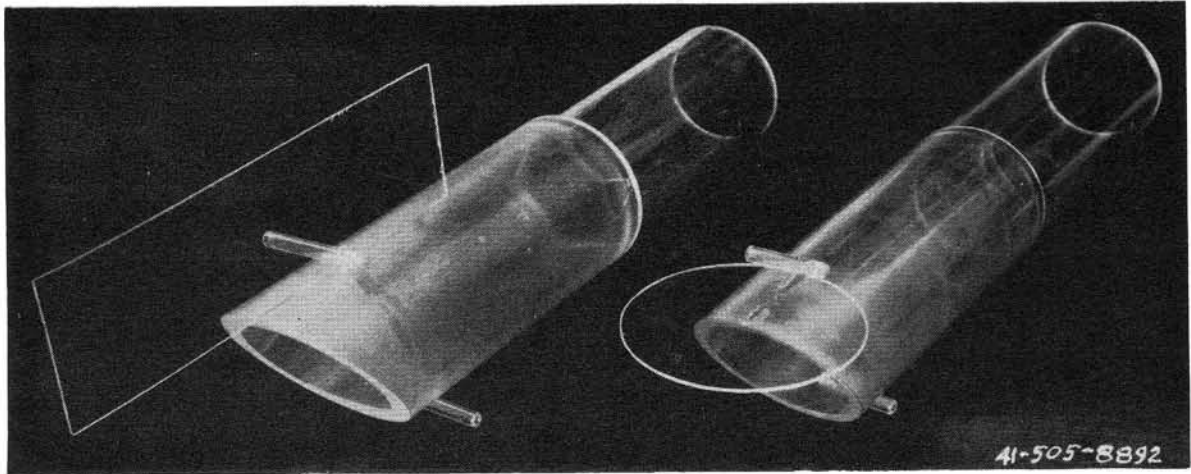


Fig. X-1 - Hood Inlet and Anti-Vortex Device.

the course of the hood inlet study. Correspondence with Mr. Meyer indicates that the hood inlet idea originated at Missouri during a discussion early in the summer of 1954 between Mr. Meyer and D. D. Smith, formerly Project Supervisor for the Soil and Water Conservation Research Division of the Agricultural Research Service at Columbia, Missouri. The hood inlet tests were so far advanced by the time the Missouri results were available that the Missouri report had no influence on the test program. However, the Missouri inlet which seemed best was tested.

Previous studies by the senior author [I-8, I-9 and Parts I through IX] extending from 1941 to the initiation of the present study in 1955 provided a general background for the hood inlet study: The hydraulic theory of closed conduit spillways was developed in Part I of this report series; the different types of flow in closed conduit spillways has been observed [I-8 and Parts I through IX]; the test apparatus was already available [I-8, Part V and Fig. X-3]; test methods had been standardized [I-8 and Part V]; and the methods of analysis [I-8 and Part V] were familiar, although they were modified and improved as a result of field laboratory experiments reported by W. O. Ree [I-42]. The previous experimental experience and the availability of the test apparatus contributed greatly to the expeditious prosecution of the hood inlet investigation.

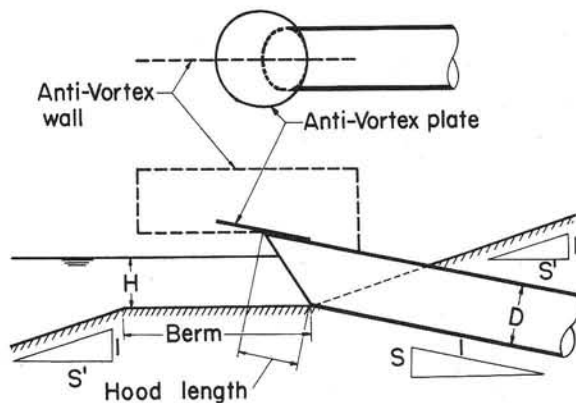


Fig. X-2 - Definition of Terms.

with a Plexiglas extension of their test conduit. Their tests were made with a level approach floor and a 2:1 embankment slope through which the inlet projected. The culvert was tested on 0, 4 and 8 per cent slopes.

The potential requirements of the Soil Conservation Service and their cooperators were given consideration in planning the experimental program. The largest numbers of hood inlets will probably be used on small farm and ranch ponds and on headwater flood detention structures since on the order of 100,000 of these ponds and reservoirs are built annually. The slope of the conduit through these dams varies over wider limits than were tested by Karr and Clayton. Furthermore, it may be desirable to project the entrance into the pond or reservoir to eliminate the possibility of scour close to the entrance. These and other practical considerations led to the development of the following program of experimental investigation.

#### EXPERIMENTAL PROGRAM

A careful study of the paper by Karr and Clayton [I-28] revealed a number of areas where further investigation would be desirable. Karr and Clayton determined the optimum hood lengths by mounting sheet metal on the outside of the pipe. The final test was made

### Hood Length

The optimum hood length was determined for the most severe conditions of installation-- thin-walled, re-entrant inlets. Hood lengths tested were OD, D/8, D/4, 3D/8, D/2, 5D/8, 3D/4, and 1D. The optimum hood lengths were initially determined for conduit slopes of 20 per cent and subsequently redetermined for conduit slopes of 0, 2.5, 5, 10, and 36 per cent.

### Conduit Slope

The performance of the hood inlet and the conduit were observed for conduit slopes varying from 0 to 36 per cent, the steepest obtainable with the test apparatus. These observations were made in connection with the hood inlet determination.

### Wall Thickness

The majority of the tests were conducted using wall thicknesses of 0.015D. However, to evaluate the effect of the thickness of the pipe wall, the wall thickness was varied from 0.012D to 0.22D in small increments for the optimum hood length. An attempt was made to test wall thicknesses of 0.006D but the inlet was so fragile it collapsed before sufficient data could be obtained.

### Entrance Shape

The hood inlet entrance was square-edged for most of the tests. Tests were made with a radius of rounding of 0.21D for hood lengths of OD and 3D/4. Difficulties of fabricating a small model of corrugated pipe prevented model tests of corrugated pipe inlets.

### Anti-Vortex Device

Vortices are known to affect the spillway performance. A number of different types of vortex inhibitors were tried out and several of those which showed promise were tested.

### Approach Conditions

Most of the tests were conducted with re-entrant entrances. However, tests were conducted with a 1 on a 3-1/3 dam face in place and with a berm on the dam to evaluate the modifying effect of these changes. The dam face was fixed in place with cement for some tests while for others a scour hole was permitted to form in the sand face of the dam.

### Scour

A series of tests was conducted using relative full pipe discharges of  $Q/D^{5/2}$  of 3, 5, 10, and 15 to determine the size of hole scoured in several sizes of sand and rock. The bed materials had mean sieve sizes of 0.006, 0.035, 0.12, 0.37, 0.63, 1.0, 1.5, and 2.0 inches.

The tests are summarized in Table X-1.

## TEST APPARATUS

The laboratory apparatus was especially designed for the closed conduit spillway study. It is the fifth experimental setup used for this study and embodies improvements based on experience with previous installations.

The approach channel is relatively large and the water enters it very quietly, providing excellent approach conditions. The conduit is supported on a heavy beam that has easy slope adjustment. The water supply is obtained from an individual recirculating pump and reservoir system. Flows are measured with multiple orifice meters. Headpool levels are recorded continuously on a chart and pressures within the conduit are recorded by photographing the manometers.

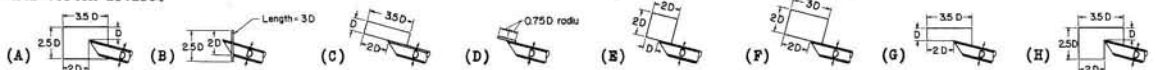
Fig. X-3 is a perspective sketch of the test apparatus.

The steel approach channel is 16 ft long, 3 ft wide, and 2 ft deep. It is simply supported at the upstream end and cantilevers over a bracket near the downstream end. The bracket is

TABLE X-1  
SUMMARY OF TESTS  
D = 0.1875 ft  $l/D = 109.94$

Series	s	z/D	t/D	Hood Length D	Entrance Edge	Anti-Vortex Device <sup>a</sup>	C <sub>o</sub>	K <sub>e</sub>	Crown		Invert <sup>b</sup> h <sub>n</sub> /h <sub>yp</sub>	Remarks
									h <sub>n</sub> /h <sub>yp</sub>	Station		
34	0.200	21.47	0.0116	0	Square	A & B	4.45	0.81	-1.72	.5D	-1.56	
35	0.200	21.49	0.0151	0.125	Square	B	4.34	0.86	-0.56	.5D	-1.66	
36	0.200	21.42	0.0151	0.250	Square	B	4.42	0.88	-0.56	.5D	-1.35	
37	0.200	21.50	0.0151	0.500	Square	B		0.93	-0.38	.5D	-0.92	
38	0.200	21.49	0.0156	0.375	Square	B		0.88	--	--	-1.09	
39	0.200	21.46	0.0156	0.736	Square	B	--	0.96	--	--	-0.64	
40	0.200	21.45	0.0156	1.000	Square	B	--	0.98	--	--	-0.66	
41	0.200	21.46	0.0147	0.625	Square	B	--	0.94	--	--	-0.77	
42	0.200	21.43	0.0572	0.731	Square	B	--	0.73	+0.57	0D	-0.80	
43	0.200	21.43	0.1165	0.729	Square	B	--	0.64	+0.45	.2D	-0.70	
44	0.200	21.43	0.2245	0.750	Square	B	--	0.75	+0.46	0D	-0.75	d
45	0.200	21.43	0.0156	0.736	Square	None	--	1.01	+0.85	0D	-0.59	
46	0.200	21.43	0.0156	0.736	Square	C	--	0.95	+0.72	0D	-0.55	
47	0.200	21.43	0.0156	0.736	Square	D	--	0.98	+0.72	0D	-0.58	
48	0.200	21.43	0.0156	0.736	Square	E	--	1.01	+0.22	0D	-0.60	
49	0.200	21.43	0.0156	0.736	Square	F	--	0.85	+0.67	0D	-0.50	
50	0.200	21.54	0.0156	0.736	Square	C	--	0.93	+0.71	0D	-0.50	e
51	0.200	21.56	0.0156	0.736	Square	C	--	0.80	+0.57	0D	-0.34	f
52	0.200	--	0.0156	0.736	Square	C	--	--	--	--	--	g
53	0.200	21.58	0.0156	0.736	Square	C	--	0.93	+0.66	0D	-0.43	h
54	0.200	21.58	0.0156	0.736	Square	C	--	0.84	+0.38	0D	-0.21	i
55	0.200		0.2080	0	Round <sup>b</sup>	C	--	0.10	-0.21	.25D	-0.32	
56	0.361	39.10	0.0147	0.749	Square	C	--	0.97	--	0D	-0.55	
57	0.361		0.0147	0.625	Square	C	--	0.92	--	--	-0.71	
58	0.361		0.0151	0.500	Square	C	--	0.94	-0.22	.5D	-0.85	
59	0.361		0.0156	0.375	Square	C	--	0.91	--	--	-1.04	
60	0.361		0.0151	0.250	Square	C	--	0.92	-0.42	.5D	-0.82	
61	0.361		0.0156	1.000	Square	C	--	1.01	--	--	-0.61	
62	0.000	-0.50	0.0116	0	Square	C	--	0.77	--	--	-1.37	
63	0.000		0.0151	0.250	Square	C	--	0.84	--	--	-1.05	
64	0.000		0.0151	0.500	Square	C	--	0.85	-0.14	.5D	-0.81	
65	0.000		0.0147	0.749	Square	C	--	0.99	+0.58	0D	-0.30	
66	0.000		0.0156	1.000	Square	C	--	1.00	--	--	-0.59	
67	0.025	2.34	0.0156	1.000	Square	C	--	1.03	--	--	-0.56	j
68	0.025		0.0147	0.749	Square	C	--	0.97	+0.81	0D	-0.75	j
69	0.025		0.0147	0.625	Square	C	--	1.05	--	--	-0.71	j
70	0.025		0.0151	0.500	Square	C	--	0.91	-0.11	.5D	-0.79	j
71	0.025		0.0156	0.375	Square	C	--	0.96	--	--	-0.94	j
72	0.025		0.0151	0.250	Square	C	--	0.91	-0.24	.5D	-1.16	j
73	0.025		0.0151	0.125	Square	C	--	0.90	-0.58	.5D	-1.52	j,k
74	0.025		0.0116	0	Square	C	--	0.78	-1.24	.5D	-1.43	j,k
75	0.050	4.96	0.0156	1.000	Square	C	--	1.00	--	--	-0.60	
76	0.050		0.0147	0.749	Square	C	--	0.98	+0.54	0D	-0.59	
77	0.050		0.0147	0.625	Square	C	--	0.94	--	--	-0.77	
78	0.050		0.0151	0.500	Square	C	--	0.94	-0.26	.5D	-0.84	
79	0.050		0.0156	0.375	Square	C	--	0.89	--	--	-0.98	l
80	0.050		0.0151	0.250	Square	C	--	0.89	-0.23	.5D	-1.24	
81	0.1011		0.0156	1.000	Square	C	--	1.01	--	--	-0.60	
82	0.1011	10.51	0.0147	0.749	Square	C	--	0.95	+0.70	0D	-0.59	
83	0.1011		0.0147	0.625	Square	C	--	0.95	--	--	-0.78	
84	0.1011		0.0151	0.500	Square	C	--	0.92	-0.20	.5D	-0.87	
85	0.1011		0.0156	0.375	Square	C	--	0.90	--	--	-1.04	
86	0.1011		0.0151	0.250	Square	C	--	0.87	+0.11	.5D	-0.44	
87	0.2029		0.2245	0.750	Square	C	--	0.826	+0.49	0D	-0.77	
88	0.2029		0.1165	0.729	Square	C	--	0.826	+0.49	.2D	-0.80	
89	0.2029		0.0572	0.731	Square	C	--	0.841	+0.53	0D	-0.82	
90	0.2029		0.2013	0.746	Square	G	--	0.813	+0.50	0D	-0.73	
91	0.2029		0.0516	0.742	Square	G	--	0.836	+0.56	0D	-0.82	
92	0.2029		0.1000	0.731	Square	G	--	0.829	+0.51	.02D	-0.78	
93	0.2029		0.0147	1.178	Square	G	--	1.289	+0.96	0D	-0.30	m
94	0.2029		0.0422	0.745	Square	C	--	0.838	+0.58	0D	-0.81	
95	0.2029		0.1819	0.750	Square	C	--	0.814	+0.53	0D	-0.75	
96	0.2029		0.0807	0.735	Square	C	--	0.804	+0.49	.02D	-0.78	
97	0.2029		0.0312	0.740	Square	C	--	0.877	+0.59	0D	-0.78	
98	0.2029		0.1615	0.748	Square	C	--	0.834	+0.50	0D	-0.78	
99	0.2029		0.0274	0.741	Square	C	--	0.919	+0.64	0D	-0.76	
100	0.2029		0.1110	0.745	Square	C	--	0.827	+0.52	0D	-0.77	
101	0.2029		0.0229	0.742	Square	C	--	0.975	+0.69	0D	-0.70	
102	0.2029		0.0106	0.734	Square	C	--	--	--	0D	--	
103	0.2029		0.2120	0.738	Round <sup>b</sup>	C	--	0.158	+0.46	.03D	-0.21	
104	0.2029		0.0116	0.745	Square	C	--	1.015	+0.70	0D	-0.54	
105	0.2029		0.0058	0.746	Square	C	--	--	--	0D	--	
106	0.2029		0.0807	0.735	Square	H	--	0.832	+0.52	.02D	-0.79	

<sup>a</sup>Anti-vortex device:



<sup>b</sup>Radius is 0.21D. <sup>c</sup>At Station 0.5D. <sup>d</sup>Recorder zero questionable. <sup>e</sup>1:3.37 dam face and scour hole. <sup>f</sup>1:3.37 dam face and fixed dam face without scour hole. <sup>g</sup>Scour tests. <sup>h</sup>1:3.37 dam face, 4.22D berm and scour hole. <sup>i</sup>1:3.37 dam face, 4.22D berm and fixed dam face without scour hole. <sup>j</sup>Conduit slope is greater and less than friction slope, depending on flow. <sup>k</sup>Conduit filled by sealing exit and exhausting air. <sup>l</sup>One prime at a very low head. <sup>m</sup>Missouri sliced inlet.

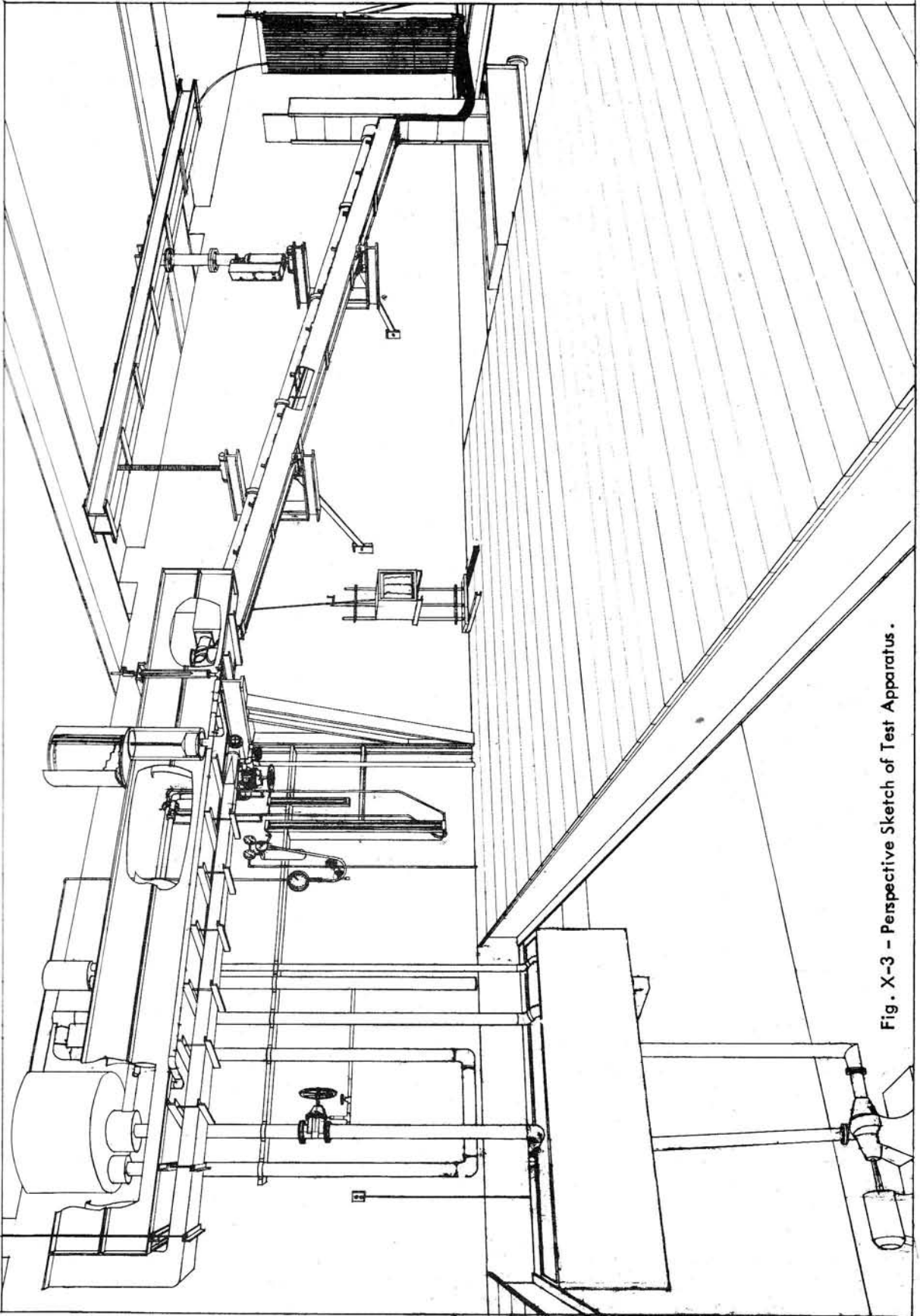


Fig. X-3 - Perspective Sketch of Test Apparatus .

located in such a position that there is no vertical movement of the downstream end of the approach channel with changes in water depth within the approach channel.

Water enters the approach channel at its upstream end and from the bottom. The expansion between the 4-in. supply pipe and the upstream end of the channel is 4 in. high and diverges from a 4-in. width to a 36-in. width in 9 ft. The combination of the long expansion, bottom entrance to the approach channel, and low velocity at the expansion exit produces excellent flow conditions in the approach channel.

The closed conduit spillway is a Lucite pipe having a nominal internal diameter  $D$  of 2-1/4 inches and a length of 20 ft 7-1/2 in. (110D). The conduit passes through the end of the approach channel, the opening being sealed by a Lucite block containing an O-ring. Couplings between each section of Lucite pipe also contain O-ring seals, providing water and air-tight joints that allow some expansion and contraction. The conduit is mounted on two laced, 6-in. steel channels 18 ft 9 in. long. Slope adjustment and support for the approach channels is provided by two 1-1/2-in. diameter screws spaced 10 ft 3 in. apart. Slopes from 0 to 36 per cent are possible.

The discharge from the conduit is collected in a 4-in. Lucite pipe and discharges into a vertical waste receiver for return to the supply reservoir. Free-flow existed at the conduit exit at all times.

The supply reservoir is a tank 8 ft 2 in. long, 4 ft 0 in. wide, by 2 ft 6 in. deep supplemented by a 12-in. pipe 27 ft 2 in. long, which is also used as part of the return piping. Borax is added to the water as a rust inhibitor.

A centrifugal pump takes water from the storage reservoir and forces it through a control valve into an individual constant level reservoir. The constant level reservoir could not be installed as high as was desirable so it was sealed and pressurized. Excess air is fed to the constant level reservoir and the excess air bled off through a pipe submerged at a constant depth below a water surface. This insures a constant head on the flow control valve at all times.

Two parallel lines take water from the constant level tank through orifice meters and control valves to the expansion below the approach channel. The 2-in. supply line contains a 1.0-in. orifice and the 4-in. supply line a 2.1-in. orifice. Pressure drop across each orifice is measured by a water manometer 50 in. long for low flows. A mercury manometer 15 in. long is used for deflections exceeding the range of the water manometer. Each orifice meter was calibrated by weighing the water discharged in a given time. The indicated precision is between 1 and 2 per cent.

The water level in the approach channel is recorded on a chart using a Stevens type M water level recorder. A natural stage scale is used and the chart speed is 36 in. per hour. Pens along each border indicate the chart width and permit corrections for chart dimension changes between the time of recording and the time of reading. The top border pen also marks each minute and the bottom border pen is also used to note events, such as the instant a photograph is taken. A point gage is installed in parallel with the water level recorder, but all heads were taken from the recorder chart because of the experimental methods employed (see section "Analytical Methods").

Piezometers are located at intervals along the conduit invert to determine the pressures within the conduit and define the hydraulic grade line. The pressures are measured by open-top water manometers grouped on a single board. The water in the manometers was colored with food dye so it could be readily seen. The manometer board is white Lucite on which lines have been scribed at 0.02 ft intervals with the aid of a milling machine. The scribed lines were dyed black using an oil dye dissolved in chloroform. Pressures at the crown at the entrance are also recorded using an Esterline-Angus bellows type pressure recorder. This is to obtain pressure fluctuations as well as to determine the minimum pressure at that point.

Photographic recording of the manometric data and the flow conditions is employed. Fluorescent lights mounted in back of white Lucite provide back lighting for the conduit. Photoflood lighting is used behind the translucent manometer board and photoflood lamps illuminate the conduit inlet. Recomar cameras are directed at the inlet, the conduit, and the manometer board. They are tripped magnetically and simultaneously from a single button. A second button pressed at the same time marks the headpool water level recorder chart and the pressure recorder chart. Photographs are taken of the manometer board for all full pipe flows. Other photographs are taken using all cameras when it seems desirable to do so. Thus, all data are permanently recorded on charts or on film except for the orifice meter readings and the notes as to flow conditions or special events.

## TEST PROCEDURE

An unusual procedure was used in conducting the tests, therefore, some explanation of it is in order. This procedure was adopted to save time and yet secure all the data required for a complete analysis. Tests covering a complete range of flow conditions were ordinarily completed in two to three hours. It would have required a minimum of one day and more likely two to three days to secure a corresponding amount of data if conventional methods had been employed.

The ordinary procedure in conducting a test of this nature is to set a rate of flow, wait until the headpool level has stabilized, and then make the observations. In the case of weir control, the headpool level stabilizes relatively rapidly. In contrast, a relatively long time is required to stabilize the flow if the control is an orifice at the entrance or a full pipe. The procedure used for these experiments involved taking all measurements "on the run," that is, before completely stabilized conditions were obtained. To accomplish this, headpool levels were taken from the water level recorder chart and all manometers were recorded simultaneously by photographing them, the instant the photograph was taken being indicated on the recorder chart. Discharges through the conduit were determined by correcting the flow to the headpool, as determined from the orifice meters, for the rate of change in the headpool storage, as determined from the slope of the headpool water level recorder trace.

Each series of tests was begun using increasing flows from run to run so the first few test runs involved weir flow control at the conduit entrance. The flow control valve was adjusted to a low discharge and the orifice meter manometers were read. The trace of the headpool level on the water level recorder chart was observed carefully. When the trace approached, but usually before it had reached, the horizontal, indicating a constant pool level, the flow control valve was opened to increase the flow somewhat and the observations were again taken. This process was repeated until the conduit was completely full and pipe flow controlled the discharge. For short hood lengths the control shifted from weir to orifice as the inlet was submerged. If this happened, the step-by-step increase of the inflow rate was continued until the conduit filled. For the longer hood lengths the entrance sealed off as the headpool level approached the hood crown and the conduit tried to flow full. Extra head created by the filling of the conduit for part of its length and lack of sufficient seal over the inlet resulted in the insufflation of air. This broke the seal at the inlet and a slug of water passed down and out of the pipe. As the inflow rate was increased, the slugs formed with increasing frequency. Eventually the conduit was full of an air-water mixture. Further increases in inflow reduced the amount of air flow until the conduit became full of water alone.

For the low weir flows, the inflow was cut off and the headpool allowed to drain. The slope of the drawdown curve was used to obtain the rate of flow. A higher degree of precision in the flow measurement was achieved than would have been possible if the flow had been determined by reading the small deflections produced by the orifice meters. Furthermore, more data were obtained than could have been obtained in a comparable period if the headpool level had been allowed to stabilize for each observation.

Ordinarily, the hydraulic grade line manometers were not photographed for part-full conduit flow that existed when the flow control was weir or orifice because no use of this data was anticipated. Similarly, the grade line manometers were not ordinarily photographed during slug flow or during periods when air was sucked through the conduit because previous experience had indicated the data would not be used. However, the pressures and the pressure fluctuations at the inlet crown were recorded on the pressure recorder for all runs.

Once the conduit was completely full of water, the inflow rate was sharply increased to raise the headpool to its maximum attainable level. The inflow rate was then adjusted to maintain approximately this level. When a sufficient length of trace of the headpool level had been obtained, the manometer board was photographed and the charts were marked at the same instant. The headpool drain valve was then opened to lower the pool level to the point where another observation was desired, the inflow valve was adjusted, and the recording process repeated. Since it was not necessary to wait for the inflow and outflow to equal each other exactly, the cycle for a complete test run ordinarily required less than five minutes.

These test methods, while somewhat unorthodox, proved completely satisfactory and reduced the length of time of each laboratory test to perhaps one-tenth of what would otherwise have been required.

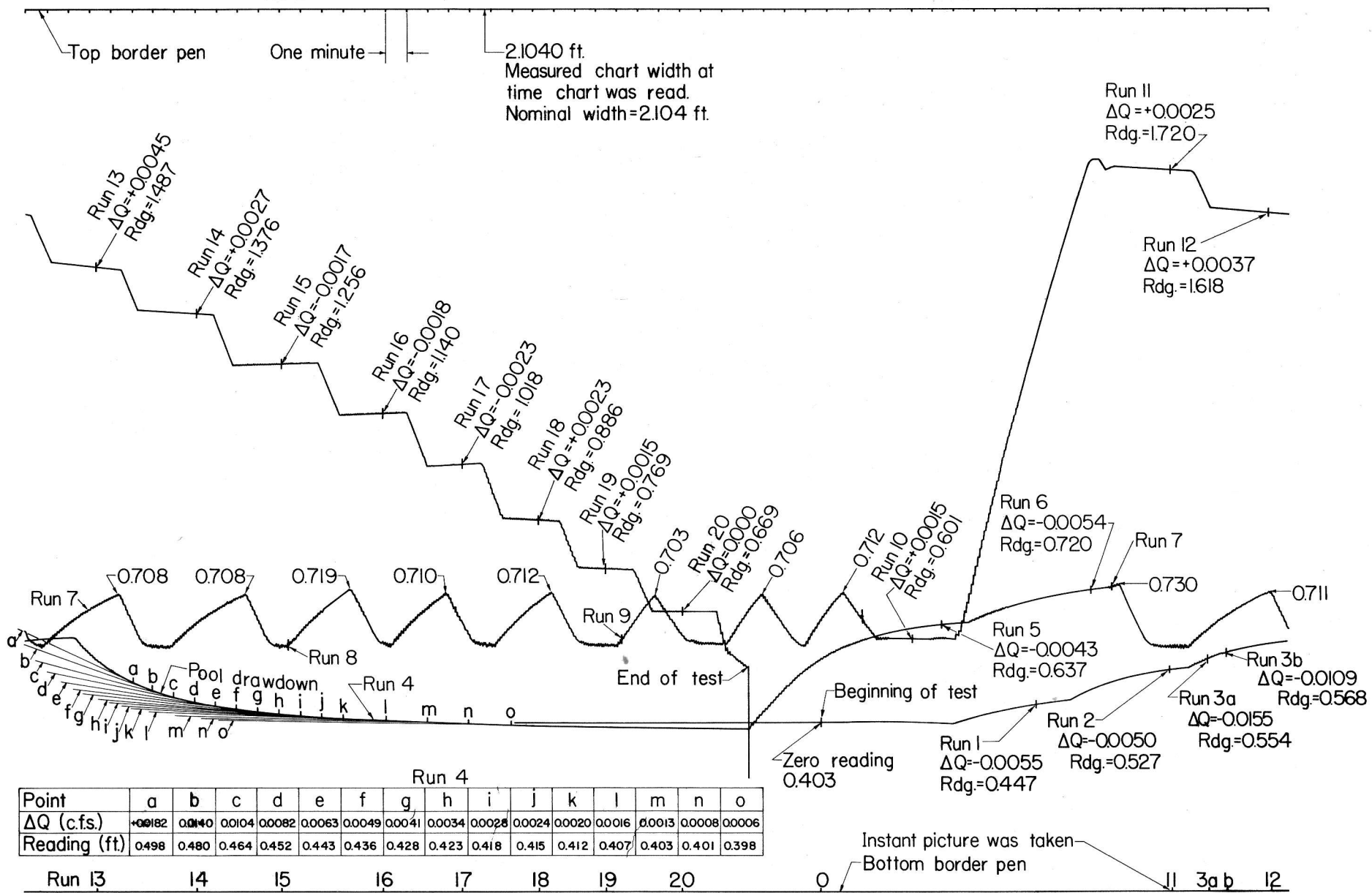


Fig. X-4 - Water Level Recorder Chart, Series 85.

## ANALYTICAL METHODS

The test methods saved a great deal of experimental time but somewhat increased the required analytical time. Nevertheless, there was a considerable net saving in overall time and more data were available for analysis.

The first step in the analysis was to take the data from the water level recorder chart. The chart reproduced in Fig. X-4 will be used for illustration although it is not from an inlet having the recommended hood length. The head and discharge for the low weir flows were obtained by marking off intervals of about one minute along the drawdown curve (Run 4, Fig. X-4), drawing tangents to the drawdown curve, determining the slope of this tangent, converting the tangent slope to rate of change of storage\*  $\Delta Q$  in cfs, measuring the height of the tangent point, and subtracting the zero reading to obtain the instantaneous head. In the case of Runs 1 and 2 of Fig. X-4, a point on the recorder trace was selected and the head reading and tangent slope in terms of  $\Delta Q$  were determined. Any other point or a number of points could have been selected. A picture was taken at Runs 3a and 3b just before and just after the headpool touched the hood crown. The chart data was read at these points. The inlet was submerged and the entrance orifice controlled the flow at the end of Run 3. Run 4 was the drawdown explained previously and was probably obtained while the observers were out to lunch. Runs 5 and 6 were made with orifice control and the chart analysis is identical to weir control. Other points along the curve could have been obtained if a better defined head-discharge curve had been desired. In fact, it is still possible to obtain additional readings from the chart.

Runs 7 to 9 were obtained for increasing flows to determine the head at which the control changed from orifice to full pipe. Only the peak heads were measured, no rate of flow data being taken from the charts. For Run 10 there was air insufflation, yet the pipe flowed continuously full of an air-water mixture. The headpool was filled between Runs 10 and 11. Runs 11 through 20 were made for full pipe flow. The point at which the headpool level and rate of change of storage were read was determined by the instant the manometer board picture was taken. This is indicated by the bottom border pen.

The data taken during the test were transferred to summary-computation sheets. This included the orifice meter readings, the water temperature, and the observational notes. The rate of inflow through the orifice meter was computed and the storage correction obtained from the recorder chart was recorded and applied to give the instantaneous rate of flow  $Q$  through the spillway. Headpool level readings were recorded and heads referenced to the inlet invert were computed.

The hydraulic grade line manometers were read by inserting the photographic negatives in a projector and projecting the image on a screen. A typical photograph is shown in Fig. X-5. The left manometer records the headpool level and its liquid surface is beyond the picture border. The next manometer measures the invert pressure near the inlet. The third and fourth tubes comprise a U-tube manometer giving the crown pressure near the inlet. From the right, the first piezometer is located  $4D$  from the conduit exit with succeeding piezometers  $8D$  intervals except that the conduit length is  $4D$  between the 12th and 13th piezometers from the conduit exit.

Elevations of the hydraulic grade line were computed from the manometric data. The grade line data were plotted and the grade lines drawn. Projection of the grade lines to the inlet and exit permitted reading the elevations of the grade line at these points. From these data were computed the grade line slope, the Darcy-Weisbach friction factor, the entrance loss coefficient, the position of the hydraulic grade line at the conduit exit, and the piezometric pressure for a hypothetical, horizontal, frictionless pipe. The procedures used for these computations were those commonly employed.

\*When  $\Delta Q$  is negative, storage is increasing; flow through spillway is less than inflow to headpool; subtract from inflow rate to obtain spillway discharge. When  $\Delta Q$  is positive, storage is decreasing; flow through spillway is greater than inflow to headpool; add to inflow rate to obtain spillway discharge.

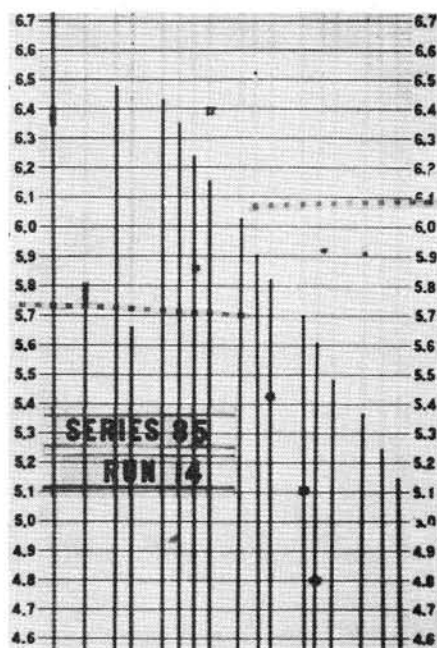


Fig. X-5 - Manometer Board, Series 85, Run 14.



The analysis of the results was possible after the computations had reached this stage.

## RESULTS OF TESTS

The hood inlet investigation was comprised of studies to: (1) determine the optimum length of the hood, (2) evaluate the effect of conduit slope on the performance, (3) develop a vortex inhibitor, (4) measure the influence of conduit wall thickness on the performance and the losses, (5) study the effect of some approach conditions, and (6) investigate the scour in the vicinity of the inlet, including riprap protection. Head-discharge curves were obtained for all variations tested and for a complete range of heads and discharges. The entrance loss coefficients for full pipe and orifice control, the weir flow rating curves, and the general performance of each variation were determined.

### Spillway Performance

The test results will, for the purposes of this paper, be presented in two sections. The first section will deal with the overall performance of the spillway. The second section will be devoted to the spillway capacity. In each section the various parts of the spillway will be discussed in turn.

### Optimum Hood Length

The optimum length<sup>∞</sup> of the hood was determined both quantitatively and by observation for six different conduit slopes. From five to eight different hood lengths were tested at each slope to evaluate the relationship between hood length and priming head. All tests were made with thin-wall, re-entrant entrances to simulate what was thought to be the most severe operating conditions. The results of these tests are summarized in Table X-2 and Fig. X-6.

The phenomena of "priming" or filling of the pipe needs to be understood in order to evaluate the results. Priming takes place when the headpool level is one or more pipe diam-

TABLE X-2  
PRIME HEADS FOR DIFFERENT HOOD LENGTHS AND CONDUIT SLOPES  
In Pipe Diameters

Conduit Slope		Hood Length							
		0	D/8	D/4	3D/8	D/2	5D/8	3D/4	D
0.000	Series No.	62 <sup>a</sup>	--	63 <sup>a</sup>	--	64 <sup>a</sup>	--	65 <sup>a</sup>	66 <sup>a</sup>
0.025	Series No.	74 <sup>b</sup>	73 <sup>b</sup>	72	71	70	69	68	67
	Maximum	5.73	5.66	3.17	1.60	1.16	1.11	1.11	1.06
	Minimum	5.55	5.42	2.75	1.14	1.08	1.09	1.04	0.96
	Average	5.63	5.57	2.90	1.47	1.10	1.09	1.06	1.02
	Events	4	3	4	9	14	21	24	19
0.050	Series No.	--	--	80	79	78	77	76	75
	Maximum			3.10	1.77	1.17	1.11	1.14	1.10
	Minimum			2.89	1.28	1.10	1.09	1.06	0.99
	Average			3.00	1.69	1.12	1.10	1.10	1.02
	Events			6	12	18	24	23	14
0.101	Series No.	--	--	86	85	84	83	82	81
	Maximum			4.72	1.93	1.33	1.17	1.17	1.16
	Minimum			2.36	1.79	1.10	1.12	1.10	1.02
	Average			3.39	1.83	1.16	1.15	1.14	1.12
	Events			8	10	13	22	42	25
0.200	Series No.	34	35	36	38	37	41	39	40
	Maximum	>6.3	>8.1	3.40	2.00	1.60	1.49		
	Minimum			3.09	1.89	1.39	1.29		
	Average			3.23	1.92	1.50	1.39	1.03	1.01
	Events	0	0	3	16	22	2	1	1
0.361	Series No.	--	--	60	59	58	57	56	61
	Maximum			4.55	2.00	1.49	1.29	1.25	1.29
	Minimum			2.86	1.87	1.43	1.29	1.23	1.27
	Average			3.57	1.91	1.46	1.29	1.24	1.28
	Events			9	10	10	2	5	13

<sup>a</sup>Inlet filled due to backwater. No priming in the sense used here.  
<sup>b</sup>Conduit filled by sealing exit and exhausting air.

<sup>∞</sup>The hood length is not measured horizontally but parallel to the conduit centerline. It is the length along the centerline between the tip of the hood and the invert at the entrance.

eters above the inlet invert and occurs somewhat differently for different hood lengths and conduit slopes.

The entrance did not prime but acted as an orifice for all heads greater than one pipe diameter when hood lengths of zero and  $D/8$  were tested with the conduit on a 20 per cent slope. This is shown in Table X-2 and Fig. X-6. The entrance contraction was so great that the conduit remained only partly full although the head on the inlet was six to eight times the pipe diameter. The priming head for these conditions is unknown but is undesirably high.

Filling of the conduit did occur for the zero and  $D/8$  hood inlet lengths when the conduit was on a 2.5 per cent slope but in a manner different than for other tests. The entrance acting as an orifice contracted the entering jet so that the velocity in the jet was greater than could be maintained with the 2.5 per cent slope. Therefore, the velocity decreased and the depth of flow increased along the length of the conduit with the water surface assuming a profile commonly designated M3. As the discharge was gradually increased, the depth of flow at the conduit exit eventually became equal to the conduit diameter, sealing off the conduit at the exit. The air trapped within the conduit was then exhausted until the conduit flowed completely full.

Filling of the pipe began at the entrance when the conduit was on a zero slope. The control was critical depth at the conduit exit and the surface profile within the conduit assumed a O2 shape. This phenomena is not the same as the priming action for conduits on steep slopes. However, the conduit did tend to fill at lower heads with a properly proportioned hood inlet than for no hood inlet or for a short hood. This filling is described in detail in a subsequent paragraph.

Priming ordinarily took place by sealing off the conduit near the inlet. The process is illustrated for a good hood inlet in Fig. X-7. The headpool level is low in Fig. X-7a so the inlet acts as a weir. Close observation shows that the water surface inside the inlet is at or very slightly above the headpool water level. The conduit is partly full as in Fig. X-8a. The head in Fig. X-7b is  $0.91D$  and "ears" are developing just inside the inlet. These ears are a local rise of the water surface that triggers the priming action. The head has increased to  $0.98D$  in Fig. X-7c and the ears have grown until they almost meet. Twenty seconds later the head had increased to  $0.99D$ , the two ears had joined together, and the inlet had primed as is shown in Fig. X-7d. In another sixty seconds the head had increased to  $1.01D$ , the inlet was completely full of water and the pipe was full for about  $1D$  as shown in Fig. X-7e.

Filling the pipe creates additional head due to the slope of the pipe. This increases its capacity. Since there is insufficient seal over the inlet, air is sucked in as shown in Fig. X-7f. Further increases in flow and head result in the formation of slugs that travel through the pipe and suck in air as shown in Fig. X-7g. These slugs are hydraulic jumps, as shown in Fig. X-8b, that form near the inlet and travel through the conduit. The slugs increase in frequency until the conduit is full of an air-water mixture as shown in Fig. X-8c. The air flow increases to a maximum and then decreases as the water flow is increased. Eventually the air flow stops, the conduit flows completely full of water as shown in Fig. X-7h, and the laws of pipe flow control the head-discharge relationship.

The distinguishing feature of the hood inlet is that the priming headpool level and the headpool level for the beginning of full pipe flow are quite low; there is little increase in head-

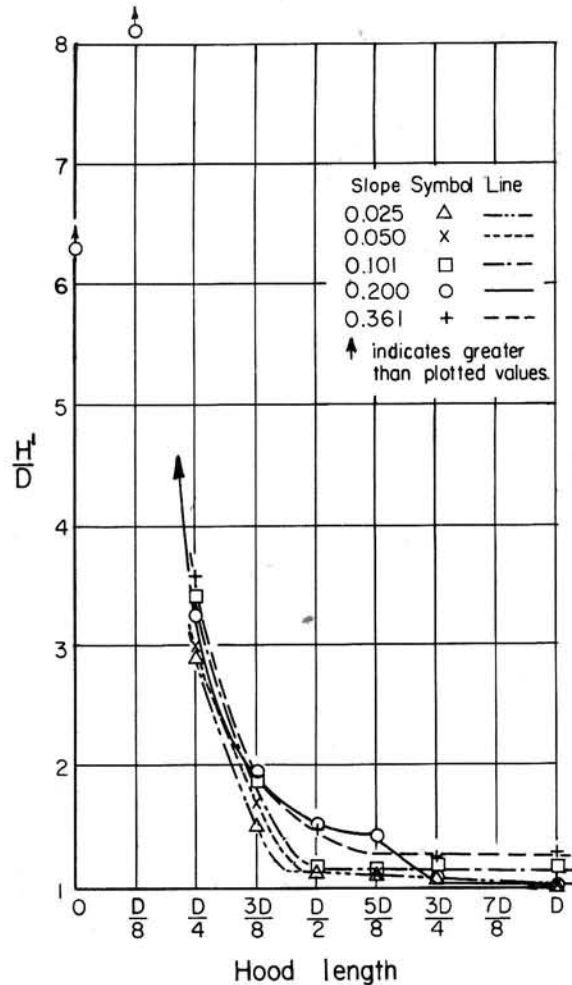
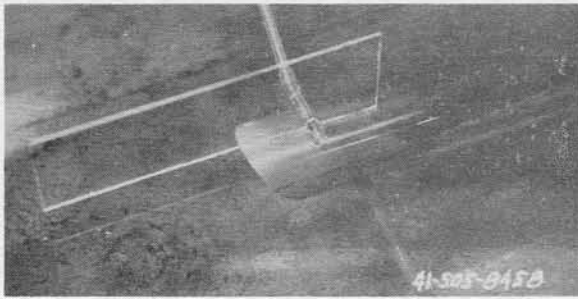
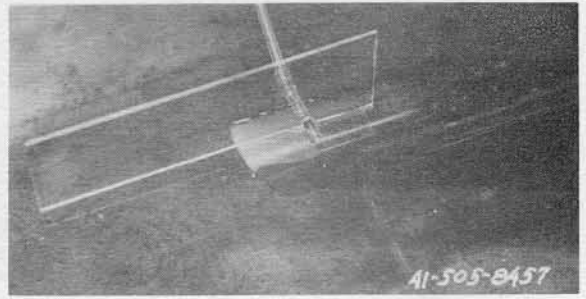


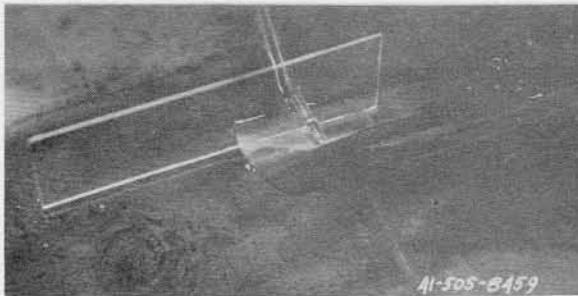
Fig. X-6 - Average Priming Head as a Function of the Hood Length.



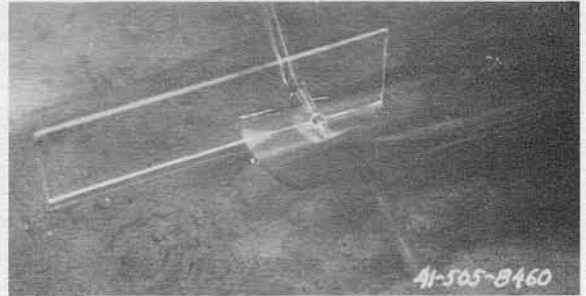
(a)  $H/D = 0.77$ . Weir flow. No ears on water surface inside inlet.



(b)  $H/D = 0.91$ . Weir flow. Ears are just beginning to appear.



(c)  $H/D = 0.98$ . Just before inlet seals. Ears from opposite sides almost meet.



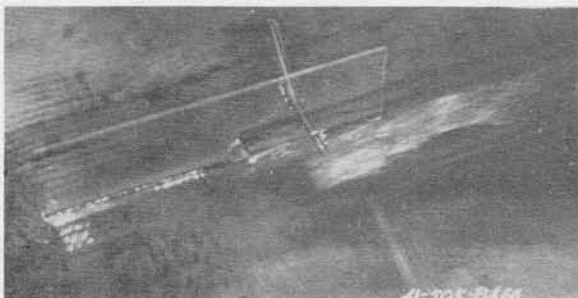
(d)  $H/D = 0.99$ . Just as inlet seals. Ears from opposite sides have joined.



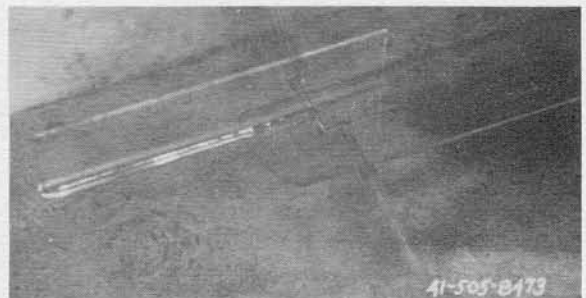
(e)  $H/D = 1.01$ . Just after inlet has sealed. There is no air entering.



(f)  $H/D = 1.08$ . Air is bubbling in. Pipe perimeter is wet about  $2D$ .

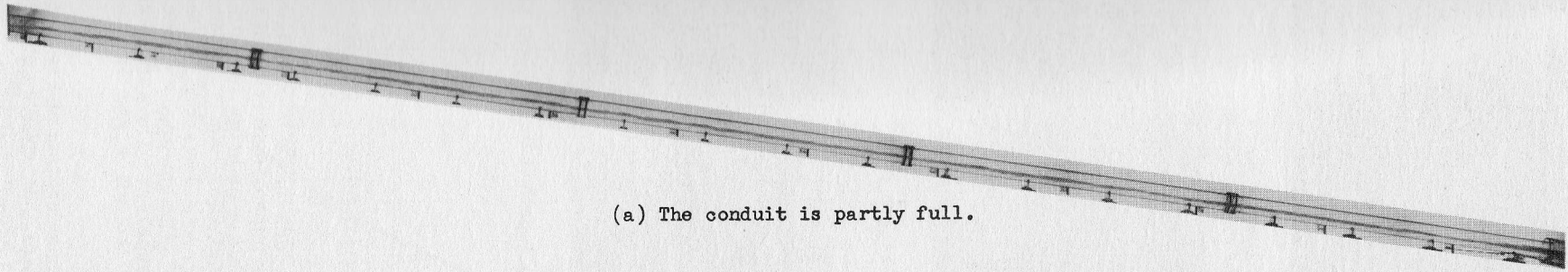


(g)  $H/D = 1.09$ . Hydraulic jump traveling through pipe and sucking air.

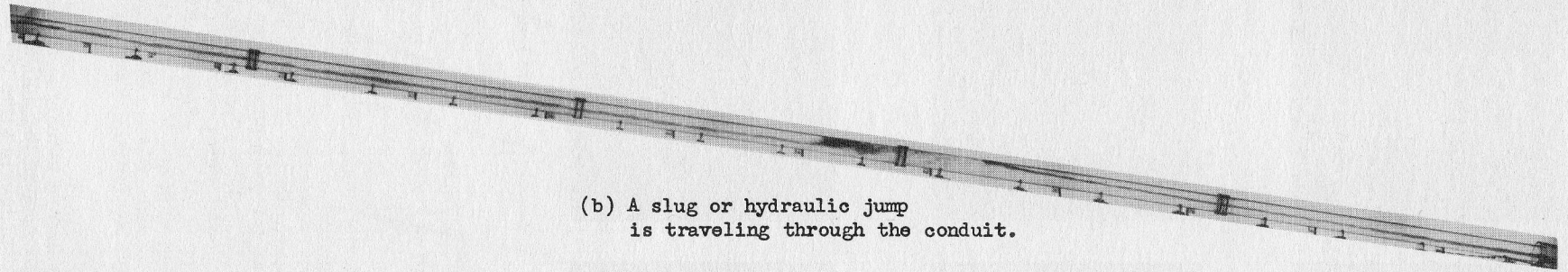


(h)  $H/D = 1.24$ . Pipe flow. No air enters inlet.

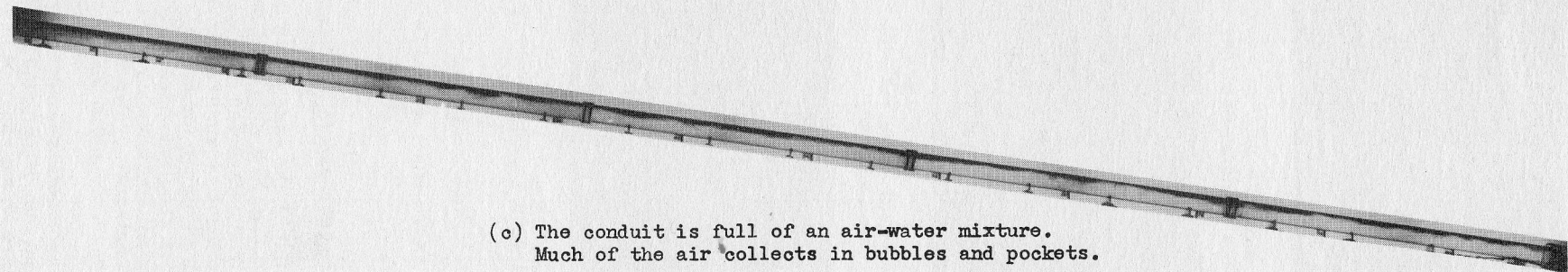
Fig. X-7 - Appearance of the Hood Inlet as the Headpool Level Rises and the Inlet Primes.



(a) The conduit is partly full.

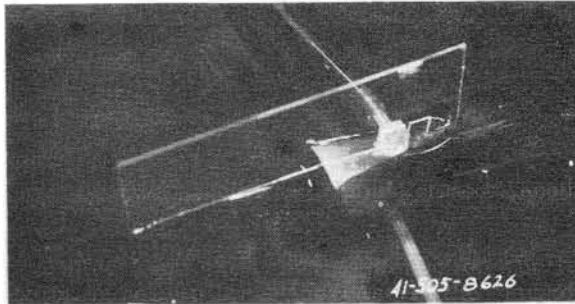
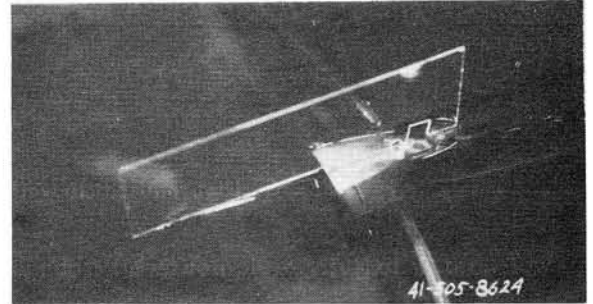
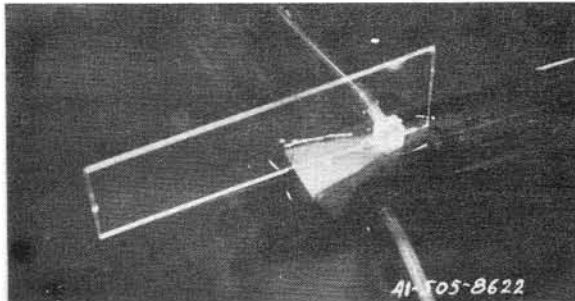
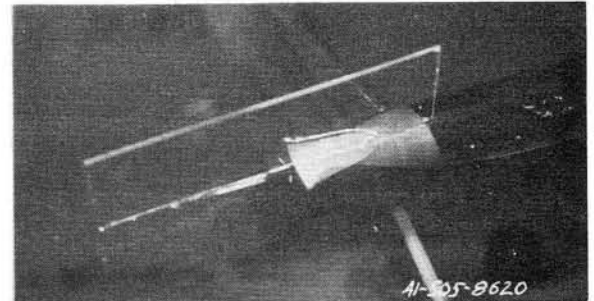
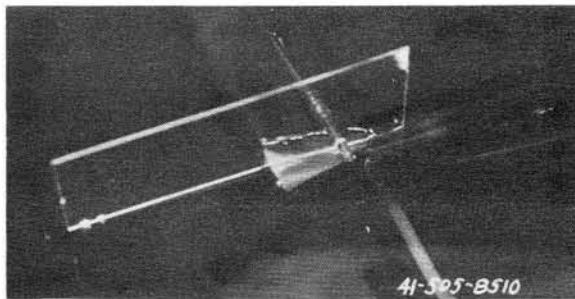
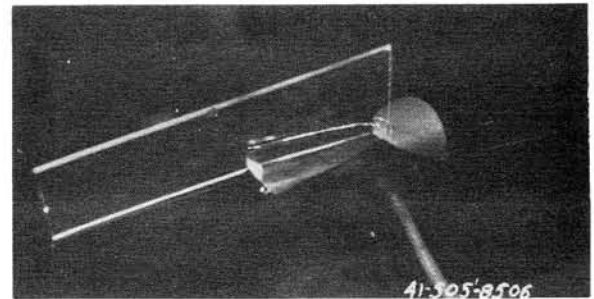


(b) A slug or hydraulic jump  
is traveling through the conduit.



(c) The conduit is full of an air-water mixture.  
Much of the air collects in bubbles and pockets.

Fig. X-8 - Some Conditions of Conduit Flow.

(a) Hood length =  $D/4$ .(b) Hood length  $3D/8$ .(c) Hood length =  $D/2$ .(d) Hood length =  $5D/8$ .(e) Hood length =  $3D/4$ .(f) Hood length =  $D$ .Fig. X-9 - Effect of Hood Length on Flow at the Inlet for  $H/D = 1.0$ .

pool level from the time the inlet primes until the conduit flows completely full of water. However, there is a large increase in the rate of flow.

The development of the ears which determine the priming depends on the hood length. This is illustrated in Fig. X-9 where the head for each photograph is approximately equal to the pipe diameter. The contracted jet expands and hits the inside wall at or below the horizontal centerline for the  $L/4$  and the  $3D/8$  hood lengths shown in Figs. X-9a and X-9b. The point of impingement is higher for the  $D/2$  hood length shown in Fig. X-9c but the air-filled entrance contraction is readily apparent. There appears to be no air in the entrance contraction for the  $5D/8$  hood length shown in Fig. X-9d. Also, ears are apparent. The ears have reached across the entrance crown and have sealed the inlet with the  $3D/4$  and  $D$  hood lengths shown in Figs. X-9e and X-9f.

A little more explanation is necessary before returning to a consideration of Fig. X-6. Although the  $D/4$  and the  $3D/8$  hood lengths caused the spillway to prime, it did so at high headpool levels. There was a range of headpool levels after the inlet became submerged for

which the control was an orifice at the entrance. The headpool level would build up, the inlet and pipe would fill, the headpool level would drop until the pipe flowed part full, and the cycle would be repeated. This is illustrated in Fig. X-4 by Runs 7, 8 and 9. The peak headpool level --the headpool level at which the inlet primes--was noted for each occurrence. This is the priming head shown in Table X-2 and Fig. X-6.

The average priming head decreases as the hood length increases until a minimum is reached at a hood length of  $D/2$  to  $3D/4$ . This is shown in Fig. X-6. There seems to be no advantage in using a hood length longer than  $3D/4$ , and this length is recommended as the minimum satisfactory length. This minimum hood length could also have been closely determined by visual observations alone, as is illustrated in Fig. X-9.

### Conduit Slope

The major effect of the slope of the conduit on the performance is in the additional head which becomes available as the slope and the total drop is increased. The effect of slope is large for the range of flows when air passes through the conduit and for full pipe flow but is small or negligible for weir control.

The slope affects the spillway performance for low discharges in the weir control range only for slopes so flat that the weir at the entrance is not the control section. This is shown in Fig. X-10 where the only weir flow control data that deviates from the composite data is that for the zero conduit slope. The low flow control for zero or very flat slopes is at the conduit exit where the weir, if one wishes to consider weir control at all, is a broad-crested weir having a length equal to the length of the conduit. (For a more detailed explanation see Part I, "Barrel Exit Control.") The rating curves for weir control will be presented later.

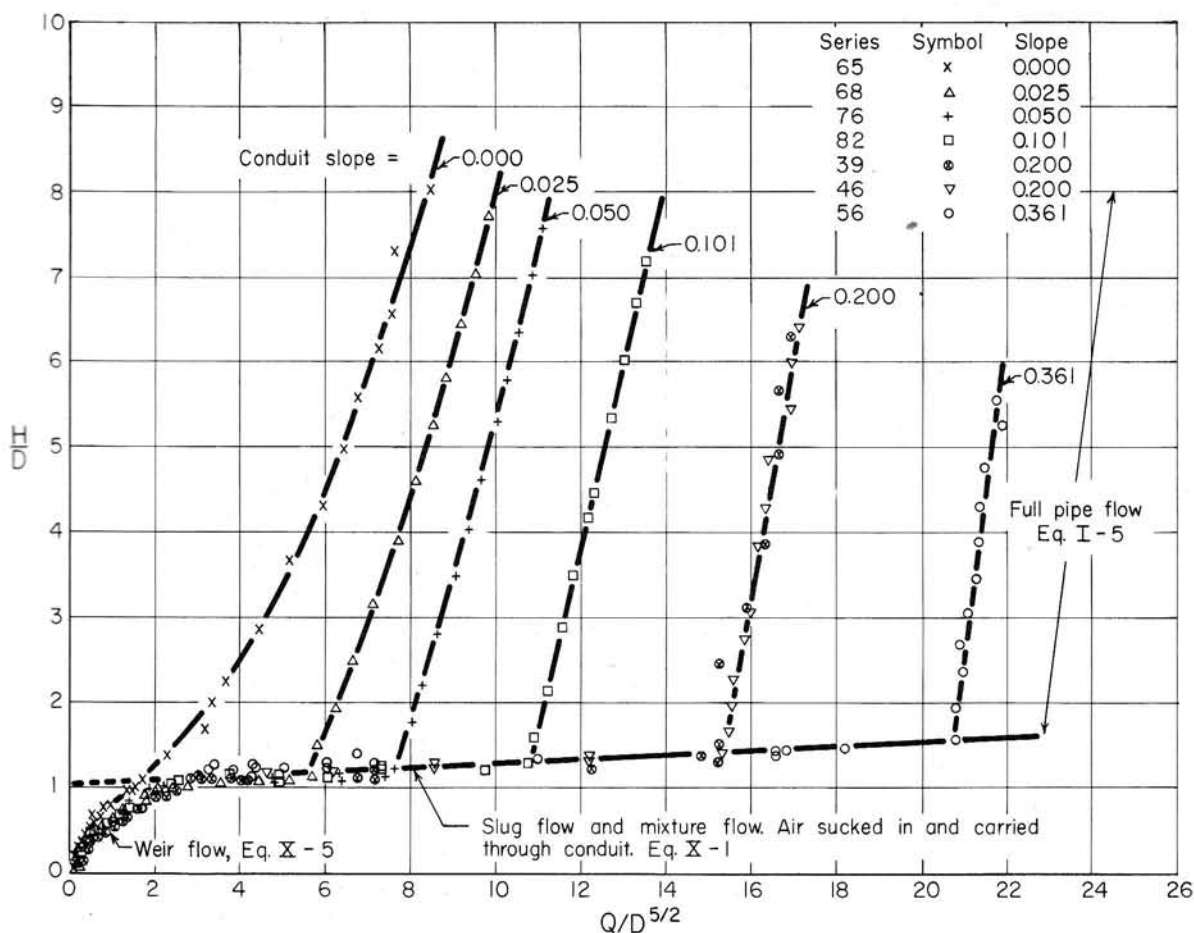


Fig. X-10 - Effect of Conduit Slope on the Head-Discharge Relationship. Hood Length is  $3D/4$ .

Orifice control exists only for the shorter hood lengths. Orifice control did not exist at all for the conduit on a zero slope because the control was at the exit for all flows and the entrance filled from backwater before orifice flow could develop. When the conduit slope was 2.5 per cent, orifice control existed up to heads sufficient to fill the pipe at the exit end, after which the conduit filled and the headpool was drawn down. Orifice control for the short hood lengths was obtained for all other slopes up to heads sufficient to cause the inlet to prime.

The full-flow discharge through the spillway increases with the conduit slope as is shown in Fig. X-10. The conduit had the same length for all slopes, so the total drop through the spillway increased with the slope. The increase in total head due to increasing the slope is actually what causes the increased flow. There was no change in the entrance loss coefficient with conduit slope.

Between weir control and full pipe control there exists a range of flows where hydraulic jumps fill the pipe and travel through the conduit as slugs or the flow is a mixture of water and air (Figs. X-8b and X-8c). Air is sucked in and carried through the conduit. Only a small amount of data were ordinarily taken from the recorder charts for this range of flows, but such data as were taken has been plotted in Fig. X-10. Two heads are plotted for some flows indicating a small fluctuation in the headpool level. This is caused by the time required for a new slug to form after the previous slug had passed out of the conduit. The range of headpool fluctuation was small for discharges a little above the point of weir control. No headpool fluctuation was observed when the slugs increased in frequency and the discharges approached that for full pipe control.

The gently sloping line in Fig. X-10 gives the head-discharge relationship for slug and air flow through the conduit. It is also a limit curve giving heads and discharges above which the control will be pipe flow. Thus, the composite head-discharge curve for a particular spillway having a good hood inlet can be drawn by plotting the weir flow curve, the slug flow curve, and the pipe flow curve. The extensions of these curves beyond their intersections with each other are imaginary so that the complete rating curve is formed by tracing, as the head and

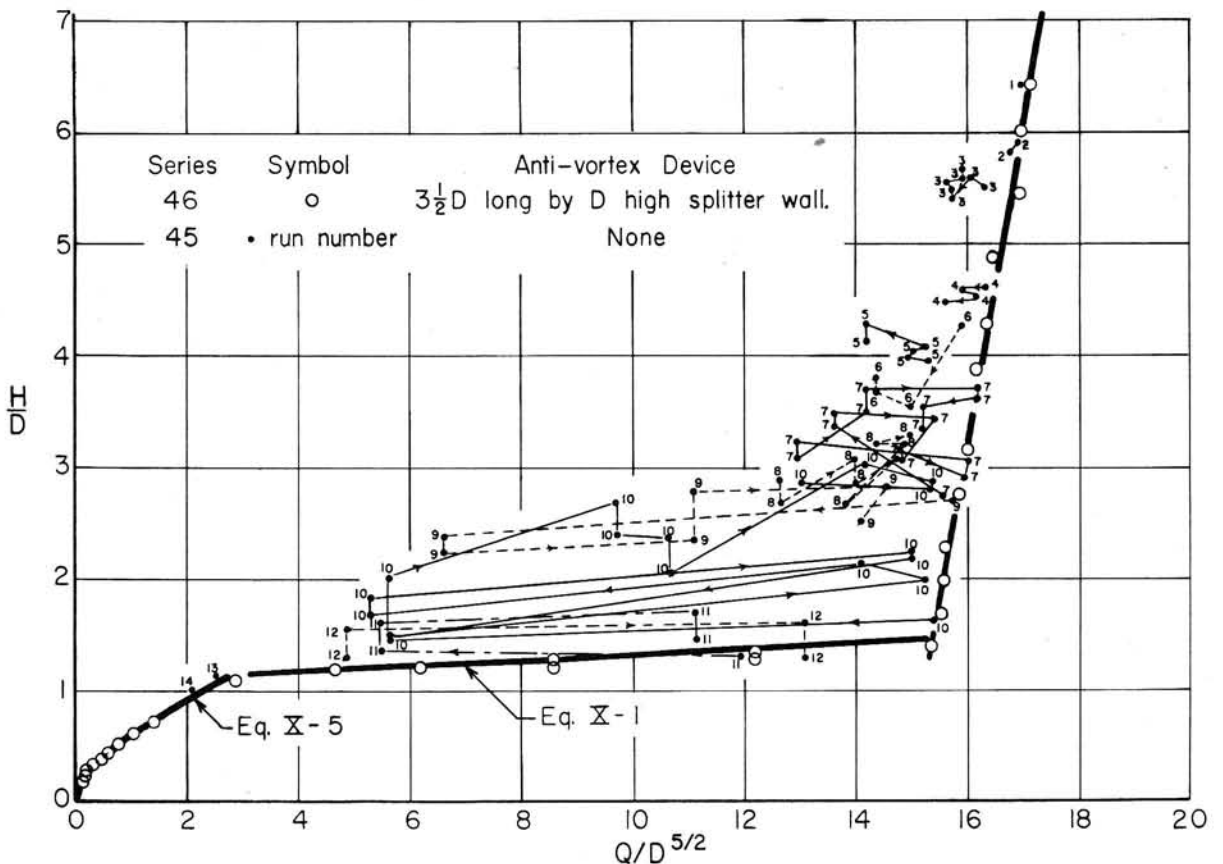


Fig. X-11 - Effect of Presence or Absence of an Anti-Vortex Device on the Capacity.

discharge increase, along the weir curve to its intersection with the slug and air flow curve, along this latter curve to its intersection with the pipe curve, and along the pipe curve for all higher heads and flows.

The equation of the slug and mixture flow curve for the  $3D/4$  hood length may be approximated by

$$\frac{H}{D} = 1.05 + 0.025 \frac{Q}{D^{5/2}} \quad (X-1)$$

The effect of slope on the performance of the closed conduit spillway is primarily a result of the additional head made available when the conduit flows full. There is no effect on the performance for part-full flow unless the slope is so flat that the conduit fills by conditions other than entrance sealing due to the entrance characteristics.

### Vortex Inhibitor

A device to control the formation of vortices at the entrance to closed conduit spillways is a necessity. The greatest need for the anti-vortex device is at low submergences of the inlet where a vortex may let air into the spillway; a vortex inhibitor is not needed for weir control at the entrance and is not essential when the inlet is deeply submerged.

The air entering through the vortex replaces the water and thereby reduces the discharge capacity of the spillway. The magnitude of the potential reduction in capacity as a result of vortices is apparent in Fig. X-11 where data are plotted for two series of tests. The open circles and the curves represent data obtained with an anti-vortex wall. The anti-vortex wall was removed for the data identified by dots and run numbers. The data obtained for each run are connected to show the order in which they were obtained. Continuous curves could have been obtained if enough points had been read from the recorder chart. However, the data plotted are sufficient to illustrate the wide variations in the discharge as the vortex strength varies.

The vortex as observed is not a steady phenomena. Sometimes there is no vortex present even though an anti-vortex device is not used, and the discharge corresponds to that obtained when an anti-vortex device is employed. At other times there may be only surface circulation or a vortex depression may develop without a deep core. At still other times a deep vortex core will extend into the inlet and admit air to the conduit. This causes a great reduction in the spillway capacity, as evidenced by the low discharges shown in Fig. X-11. Then the vortex may disappear and the discharge approximate the maximum.

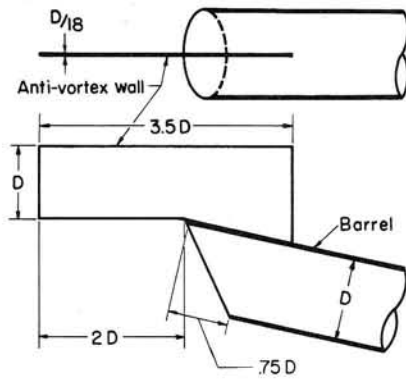
The discharge is unpredictable either in magnitude or at any given time when vortices are present. In contrast, the completely reliable and predictable head-discharge curve shown in Fig. X-11 can be obtained if an anti-vortex device is used. Since the capacity of the spillway of Fig. X-11 was reduced to only one-third its potential capacity by the elimination of the anti-vortex device, the importance of using some type of anti-vortex device is amply demonstrated. The anti-vortex device used for each series is indicated in Table X-1.

The anti-vortex device used during the series plotted in Fig. X-11 is a splitter wall mounted on the outside crown of the inlet shown in Fig. X-12a. This anti-vortex wall or the alternate shown in Fig. X-12b were used throughout most of the test program with uniformly satisfactory results. Although vortices sometimes formed, they admitted air to the conduit only briefly. These are the smallest walls that adequately inhibited vortices. Larger walls seem to have little additional benefit.

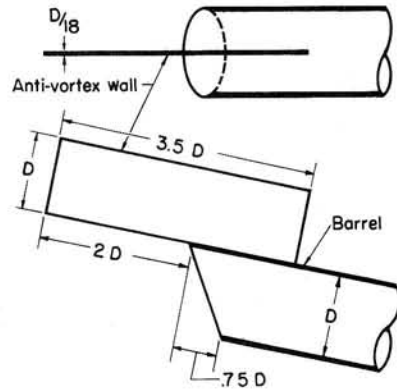
To support the upstream end of the wall it may be desirable to extend the wall downward into the approach fill. The extensions shown in Figs. X-12c and X-12d were tested with the results shown in Fig. X-13. For full pipe flow there was no difference in performance although the entrance loss was slightly increased. The weir and slug flow data indicate that the extensions did reduce the capacity somewhat. The headwall type of anti-vortex device shown in Fig. X-12e permitted much stronger vortex activity and more air entered the conduit than for the splitter type of anti-vortex device. However, the data plotted in Fig. X-13 do not indicate serious effects on the head-discharge curve. The entrance loss coefficient is less for the headwall anti-vortex device, probably due to its effect in reducing the entrance contraction. The weir and slug flow data plot with the data obtained for the Fig. X-12a anti-vortex device.

Objections to the splitter type anti-vortex wall were voiced before the tests were completed and a flat plate was suggested by Paul Jacobson, Soil Conservation Service State Eng-

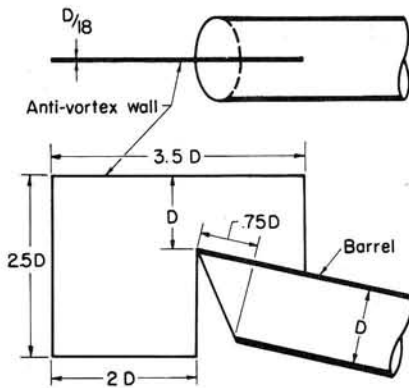




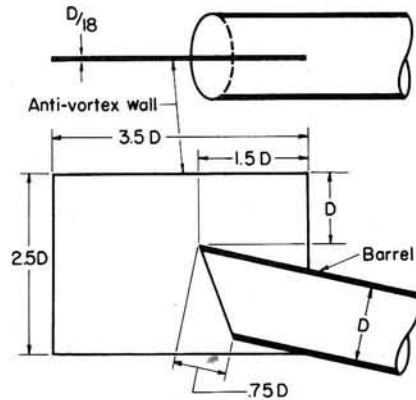
(a) Minimum Splitter Type Anti-vortex Wall.



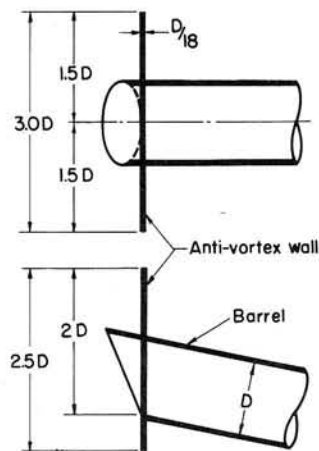
(b) Alternate Location of Minimum Splitter Type Anti-vortex Wall.



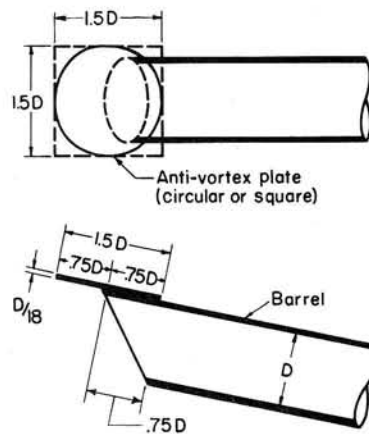
(c) Splitter Type Anti-vortex Wall with Vertical Extension.



(d) Splitter Type Anti-vortex Wall with Extension Fitted to Inlet.



(e) Headwall Type Anti-vortex Wall.



(f) Anti-vortex Plate.

Fig. X-12 - Anti-Vortex Devices.

inner for Iowa. Observational tests showed that the minimum size of anti-vortex plate is that dimensioned in Fig. X-12f. The results of a test with a flat plate anti-vortex device are presented in Fig. X-13. The pipe wall thickness is different for this test than for the previous tests so the curves cannot be compared. For this reason comparative data are plotted as pluses. Although the flat plate anti-vortex device seems fully as effective as a splitter wall anti-vortex device, it received only one test compared to the many tests for the splitter wall. The flat plate may be either circular or square as long as the minimum dimensions are those given in Fig. X-12f.

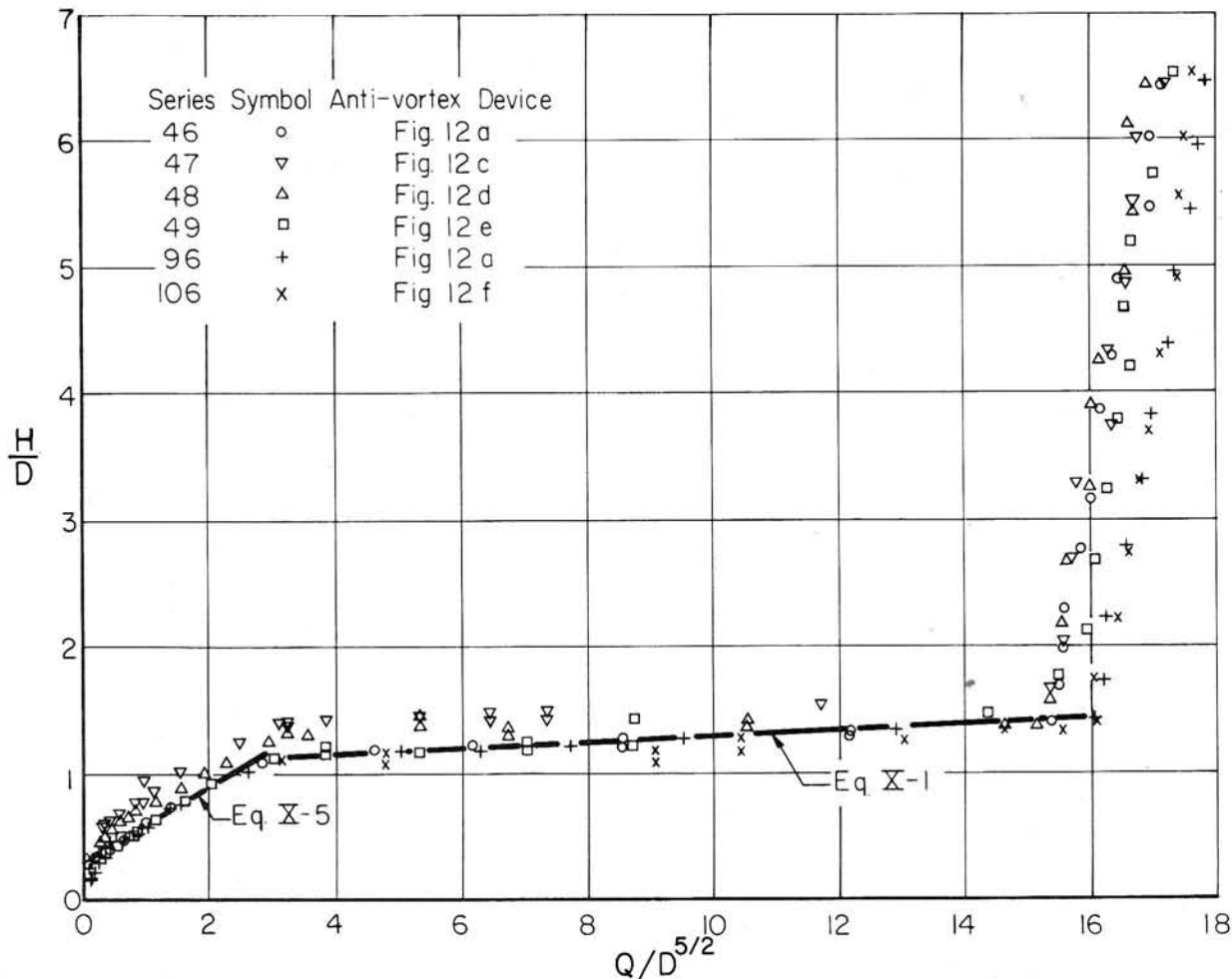


Fig. X-13 - Comparison of Head-Discharge Curves for Different Anti-Vortex Devices.

#### Conduit Wall Thickness

A wide range of pipe wall thicknesses was tested with the  $3D/4$  hood inlet length and 20 per cent conduit slope. The thickness of the thickest wall tested was  $0.224D$ . This is somewhat thicker than concrete pipe having the greatest relative wall thickness as specified by the American Society for Testing Materials. The thinnest pipe wall was  $0.015D$  thick. Attempts were made to test wall thicknesses of  $0.011D$  and  $0.006D$  but the Lucite model was so thin (0.024 in. and 0.013 in., respectively) that the inlets broke before data could be obtained. Even these thin walls are relatively thicker than the walls of metal pipe. Seventeen different wall thicknesses were tested.

The wall thickness had no apparent effect on the priming action or general inlet performance. Wall thicknesses did affect the loss at the entrance. The magnitude of this effect is described in a later section.

### Special Inlets

Three special inlets were tested so their characteristics could be compared with the recommended hood inlet. These were a sliced inlet, a well-rounded re-entrant (inwardly projecting) inlet without a hood, and a well-rounded re-entrant hood inlet.

**Sliced Inlet.** The proportions of the sliced inlet which were tested are shown in Fig. X-14a. These were selected as representing the best proportions of the type of inlet reported by Beasley and Meyer [I-4]. The proportions were subsequently confirmed through correspondence with Mr. Meyer.

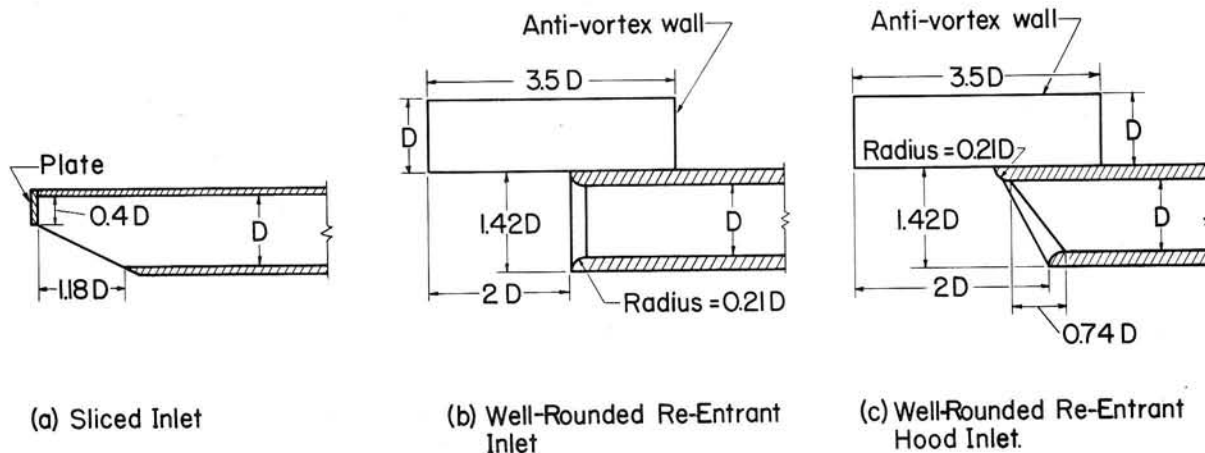


Fig. X-14 - Proportions of Special Inlets.

The results of the tests are shown as crosses in Fig. X-15. Comparative hood inlet data are shown as open circles.

The sliced inlet has some characteristics that require explanation. The sliced inlet primed in the same manner as the hood inlet shown in Fig. X-7. The inlet plate had no beneficial effect on the priming. However, once primed, the pipe continued to flow full until the headpool level dropped below the bottom edge of the inlet plate and air was admitted to the spillway. This caused a considerable headpool fluctuation at values of  $Q/D^{5/2}$  in the vicinity of 4, the magnitude of the fluctuation being about  $0.25D$ . These large fluctuations seem undesirable. Air and water pass through the conduit continuously at higher discharges and the headpool level is maintained at a relatively low level until the air flow stops and the conduit flows completely full of water. The entrance losses are high for this inlet and it had the least full-flow capacity of any of the inlets shown in Fig. X-15. As regards vortex tendencies, some type of anti-vortex device is needed to prevent the formation of strong vortices through which considerable air was observed to enter the inlet. The data shown in Fig. X-15 do not reflect the effect of vortices because they were taken when vortices were small or absent.

It appears that the sliced inlet has no significant advantage over the hood inlet and that the inlet plate may cause undesirable fluctuations of the headpool at some discharges. In any case, the development of some type of anti-vortex device is necessary before the inlet is adopted for field use.

**Well-Rounded Re-entrant Inlet.** Straub, Anderson, and Bowers [I-50] have reported tests on a well-rounded culvert entrance that indicates excellent performance. Their inlet was located in a headwall and had a radius of rounding of  $0.15D$ . The theoretical contraction coefficient  $C_c$  for the headwall entrance is  $0.611$  [I-22] and the theoretical radius of rounding is  $0.140D$  according to the equation

$$\frac{D}{2} \left[ \sqrt{\frac{1}{C_c}} - 1 \right]$$

which was developed after Harris [I-22]. This is close to the value used by Straub, Anderson, and Bowers. The contraction coefficient for a re-entrant entrance is 0.50 and the corresponding radius of rounding is 0.207D. The radius of rounding of the well-rounded, re-entrant inlet was therefore made 0.21D. A splitter anti-vortex wall was used with this inlet. The proportions of the inlet are shown in Fig. X-14b.

The results of the tests are shown in Fig. X-15 as pluses.

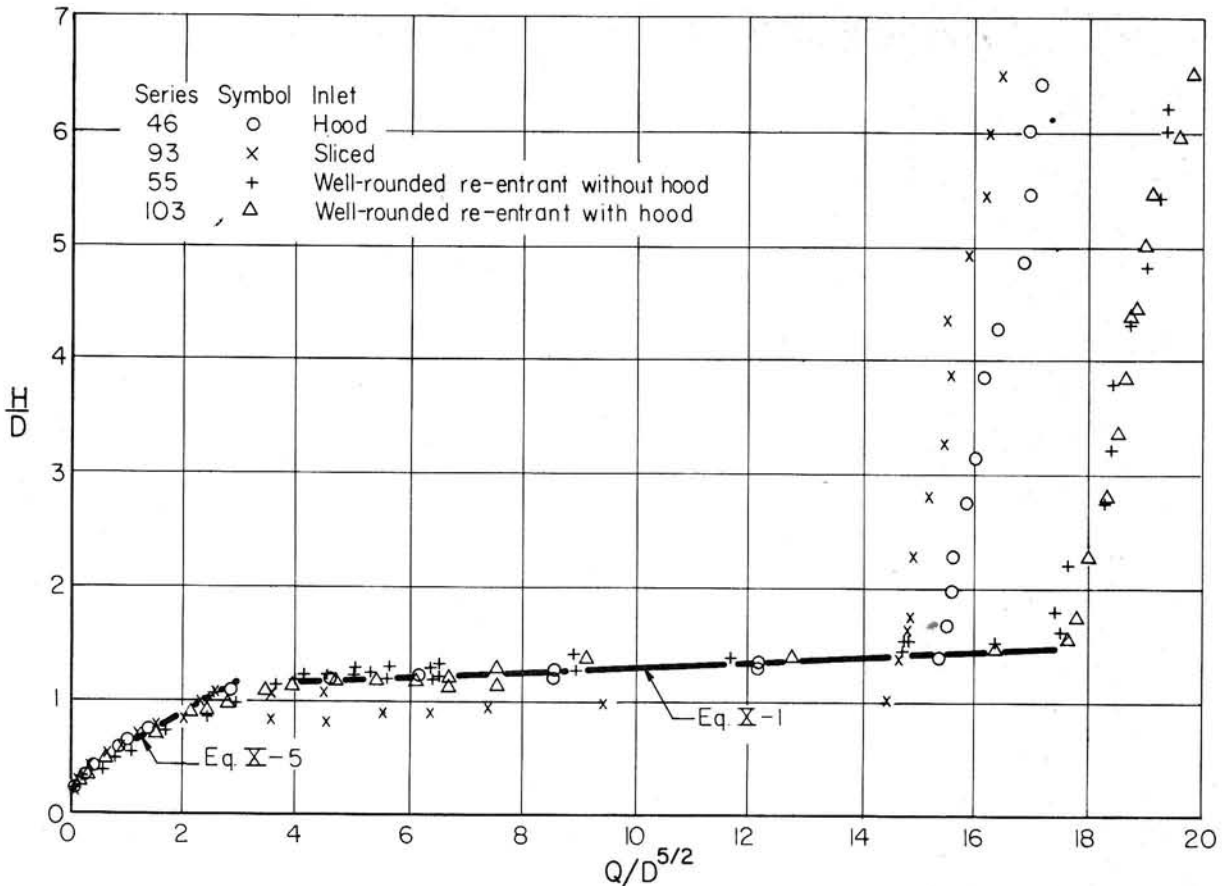


Fig. X-15 - Head-Discharge Curves for Special Inlets.

The well-rounded re-entrant inlet without a hood causes the conduit to prime at heads almost as low as does a properly proportioned hood inlet. The entrance loss coefficient is also very low. The other characteristics of the well-rounded inlet are similar to those for the hood inlet. The advantage of the hood inlet is its simplicity. The advantage of the well-rounded re-entrant inlet without a hood is its low loss coefficient. Otherwise, the characteristics of the two inlets are almost identical.

**Well-Rounded Re-entrant Hood Inlet.** A radius of rounding of 0.21D was added to the hood inlet to reduce the relatively high entrance losses. The inlet on which tests were made is shown in Fig. X-14c.

The results of the tests are shown in Fig. X-15.

The entrance loss for the well-rounded hood inlet was considerably less than for the square-edged hood entrance inlet and a little greater than for the well-rounded inlet without a hood. Otherwise, the characteristics of these three inlets are almost the same.

### Approach Conditions

A limited number of different approach conditions were tested. As noted previously, most tests were conducted with the inlet re-entrant, that is, projecting into the headpool since this was assumed to be the most severe test of the inlet performance. The inlet performance was checked with the inlet invert intersecting the sloping face of a dam and with a berm on the dam at the inlet invert elevation. The face of the dam had a slope of 1 on 3.37 and the berm had a width of 4.22D. Two conditions of each dam shape were tested: For one condition erosion was prevented by plastering the sand dam with neat cement mortar; for the other condition a scour hole was allowed to develop under maximum flow and the test was run with the scour hole.

The various approach conditions had no effect on the general performance of the spillway although the presence of the dam did reduce the entrance loss somewhat. The range of approach conditions tested is limited and deserves further study. Nevertheless, unless the approach is greatly restricted, it appears that approach conditions will not have a major effect on the general priming characteristics or the type of flow in the spillway.

### Scour at Hood Inlet

The velocity at the sharp-edged inlet is theoretically infinite. It is only logical to expect scour in the vicinity of the inlet if the material there is erodible. Fortunately, the velocity decreases rapidly with distance away from the inlet and this limits the size of the scour hole

TABLE X-3  
SIZES OF BED MATERIAL USED  
FOR SCOUR TESTS

Sand	Sieve Opening-in.		Assumed Mean Size		
	Passed	Retained	mm	in.	pipe dia.
A	See Fig. 16		0.90	0.035	0.016
B	See Fig. 16		0.15	0.006	0.0026
C	See Fig. 16		2.95	0.116	0.052
D	1/2	1/4	9.5	3/8	0.17
E	3/4	1/2	16	5/8	0.28
F	1-3/4	3/4	25	1	0.44
G	1-3/4	1-1/4	38	1-1/2	0.67
H	2-1/2	1-1/2	51	2	0.89

to a tolerable amount. A series of tests was performed to evaluate the dimensions of the hole that would be scoured in various sizes of noncohesive materials. A second objective of these tests was to determine the size of riprap required to prevent scour. And a third objective was the determination of the height of the hood inlet above the erodible material at which no scour would occur. These objectives were achieved by conducting tests at four different discharges on eight different sand sizes. The sands used as bed material were quite uniform in size, as indicated by the logarithmic-probability plots of the finer sands shown in Fig. X-16. Sand B was a natural sand having a mean size of 0.15 mm. Sand A had a mean size of 0.90 mm with most of the particles falling between the No. 16 and the No. 30 sieves. Sand C had a mean size of 2.95 mm with essentially all particles passing the No. 4 sieve and being retained on the No. 8 sieve. Sand D passed through a sieve having 1/2 in. square openings and was retained on a sieve having a 1/4 in. square opening. The assumed mean size was 3/8 in. or 9.5 mm. Similar sieves were used for the other sands. Only a few stone of this and larger sizes were needed so they were carefully selected for uniformity and shape, the shape being as nearly spherical as was possible to obtain in the natural gravel available. The sieve openings and the assumed mean sizes of all bed materials are given in Table X-3.

The selected bed material was placed in the vicinity of the inlet and a selected flow was run through the spillway until the scour hole dimensions had become stabilized. The headpool was then drained and the depth, width and length of the scour hole were measured. The next higher flow was then turned on without filling in the scour hole. After the scour hole dimensions had stabilized the flow was again turned off and the dimensions of the hole were again measured. All flows were run with the spillway full and the headpool level about 1.5D above the inlet invert. The headpool level and the flow through the spillway were controlled by a plug valve temporarily inserted at the conduit exit. This procedure was adopted to give approximately the maximum velocities in the vicinity of the inlet for the design discharge.

The scour hole dimensions in terms of the pipe diameter are given in Table X-4. The surface radius of the scour hole  $\pm r$  is plotted in Fig. X-17. In the case of the berm, the radius is taken as one-third the sum of the scour hole width and upstream length. When there was no berm, the radius is taken as one-half the width of the scour hole. Variation in the results is to be expected. The remarkable thing about Fig. X-17 is that the variation is small enough

$\pm r$ ,  $d$ ,  $d_1$ , and  $y$  are measured in the same units as the pipe diameter  $D$ , i.e., all are measured in feet or all are measured in inches.

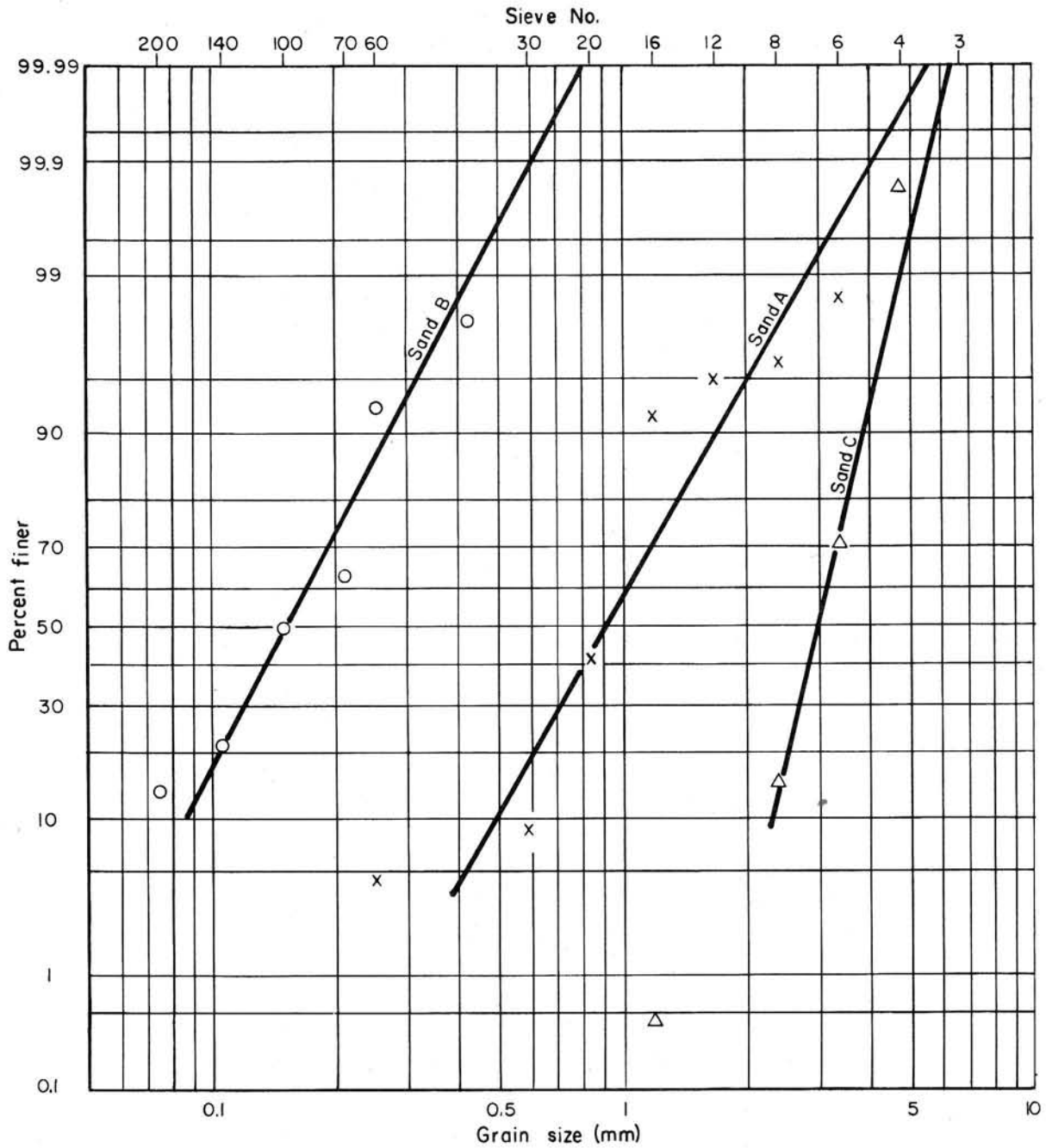


Fig. X-16 - Size Distribution of Sands Used for Scour Tests.

so reasonable curves can be drawn through the data. The curve for  $Q/D^{5/2} = 15$  is quite well defined. The same slope was used for the other values of  $Q/D^{5/2}$ . This slope fits the data as well as any other slope. The slope of the curve is  $1/5$ . By inspection, the equation of the curves of Fig. X-17 is

$$\frac{r}{D} = \left[ 0.15 + 0.04 \frac{Q}{D^{5/2}} \right] \left[ \frac{D}{d} \right]^{1/5} \quad (\text{X-2})$$

where  $d$  is the actual bed material size $\pm$ .

TABLE X-4  
SCOUR HOLE DIMENSIONS  
In Pipe Diameters

Sand	Q D <sup>5/2</sup>	Width			Length			Depth
		Right	Left	Total	Up- stream	Down- stream	Total	
(a) With berm								
B	3	0.80	0.80	1.60	0.85	0.48	1.33	0.48
	5	1.07	1.07	2.14	2.13	0.91	3.04	0.64
	10	--	1.76	3.52	1.87	1.17	3.04	0.85
	15	2.61	2.03	4.64	2.61	1.49	4.10	1.07
A	3	0.53	0.53	1.06	0.27	0.32	0.59	0.11
	5	0.80	0.69	1.49	0.80	0.53	1.33	0.27
	10	1.28	1.28	2.56	1.33	0.80	2.13	0.48
	15 <sup>a</sup>	1.65	2.08	3.73	1.87	1.07	2.94	0.69
	15 <sup>b</sup>	1.87	1.97	3.84	2.13	1.07	3.20	0.75
C	3	Scour was only 10 grains						0.21
	5	0.80	0.80	1.60	0.64	0.21	0.85	0.21
	10	0.80	0.80	1.60	0.64	0.48	1.12	0.21
	15	1.28	1.28	2.56	1.07	0.80	1.87	0.32
D	3	No movement						
	5	Two grains close to inlet invert						
	10	0.80	0.80	1.60	0.80	0.27	1.07	0.21
	15	1.07	0.96	2.03	1.07	0.75	1.82	0.37
E	5	No movement						
	10	0.53	0.53	1.06	0.59	0.00	0.59	0.32
	15	1.01	1.01	2.02	0.91	0.48	1.39	0.37
F	10	No movement but imminent						
	15	1.07	0.80	1.87	0.90	0.53	1.43	0.59
G	15	No movement but imminent						
C	10	No movement <sup>c</sup>						
(b) Without berm								
B	3	0.80	0.80	1.60	0.48	--	--	0.27
	5	0.85	0.85	1.70	0.96	0.80	1.76	0.48
	10	1.33	1.33	2.66	1.22	1.12	2.34	0.56
	15	2.24	2.24	4.48	1.81	1.44	3.25	0.90
A	3	No movement						
	5	0.27	0.27	0.54	0.27	0.32	0.59	0.21
	10	1.07	1.07	2.14	0.48	0.91	1.39	0.32
	15	2.13	2.13	4.26	0.85	1.01	1.86	0.37
C	3	No movement						
	5	About 5 grains close to inlet invert						
	10	0.80	0.80	1.60	0.43	0.21	0.64	0.16
	15	1.28	1.28	2.56	0.64	0.69	1.33	0.27
D	5	Three grains close to inlet invert						
	10	0.59	0.59	1.18	0.43	0.16	0.59	0.16
	15	0.80	1.17	1.97	0.43	0.75	1.18	0.27
E	10	Two grains close to inlet invert						
	15	1.07	1.07	2.14	0.64	0.37	1.01	0.27
F	10	No movement but imminent						
	15	1.17	0.27	1.44	0.59	--	--	0.43
G	15	One stone 1-1/2" (0.67D)						
	15	One stone 1-3/4" (0.78D)						
H	15	No movement but imminent						
C	10	No movement <sup>d</sup>						

All scour dimensions are referenced to the invert at the inlet.

<sup>a</sup>Anti-vortex wall as in Fig. 12c.

<sup>b</sup>Anti-vortex wall as in Fig. 12a.

<sup>c</sup>Berm is 0.37D below inlet invert.

<sup>d</sup>Dam face is 0.37D below inlet invert.

The data given in Table X-4 can be used to determine the grain size of the bed material which will just be picked up<sup>±</sup>  $d_1$  by a given discharge. These data are plotted in Fig. X-18 for those flows when only a few grains were picked up or for which movement was classified as imminent. A surprisingly well-defined curve is obtained which, for the data available, applies to grains of 3 mm or greater diameter. This curve has the equation

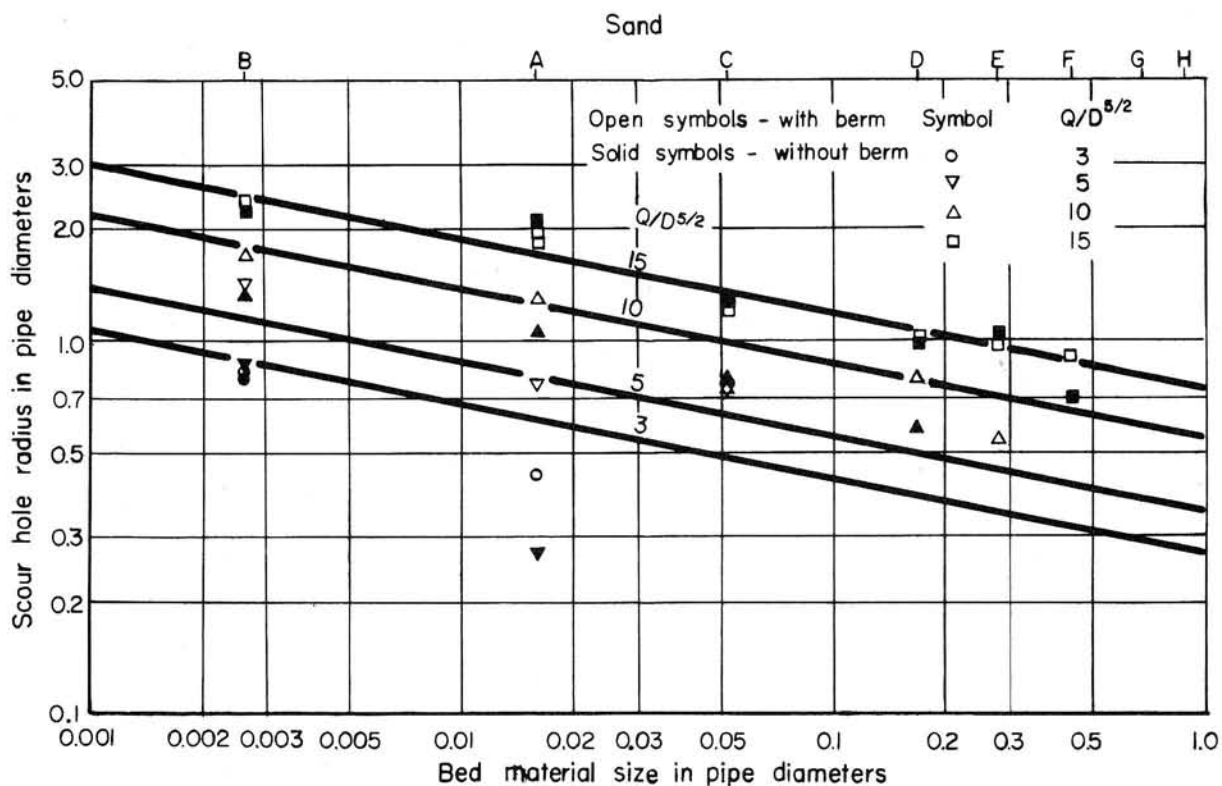


Fig. X-17 - Scour Hole Radius.

$$\frac{d_i}{D} = \frac{1}{20} \times \frac{Q}{D^{5/2}} - 0.075 \tag{X-3}$$

The depths of the scour holes<sup>±</sup> y listed in Table X-4 are plotted in Fig. X-19. Although there is considerable scatter to the data, this is not unexpected. The curves drawn in Fig. X-19 were started at the zero depth of scour as given by Eq. X-3. The slope of the curves was determined by the better defined data obtained for the two smallest grain sizes. The same slope was used for all curves. The curves of Fig. X-19 define the depth of the scour hole and have the equation

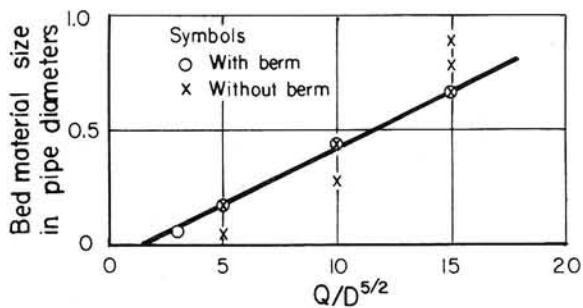


Fig. X-18 - Grain Size for Imminent Movement.

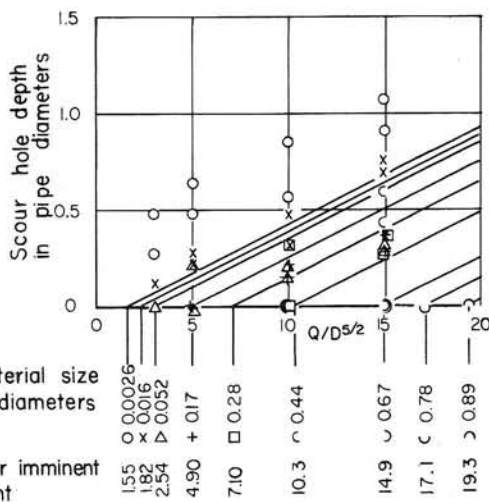


Fig. X-19 - Scour Hold Depth.



$$\frac{y}{D} = \frac{1}{20} \times \frac{Q}{D^{5/2}} - \frac{d}{D} - 0.075 \quad (\text{X-4})$$

Eq. X-4 gives fair results for bed material sizes of 3 mm or greater. The precision of this equation is low but it may serve as an aid to judgment.

Eqs. X-2, X-3 and X-4 represent the data. An ample safety factor should be used for design purposes. For example, a stone 0.89D in size was picked up when slightly disturbed. It passed through the pipe and smashed the inlet. The stone was heavy, having a specific gravity of 2.9. This points out the necessity of using riprap of adequate size, of paving to prevent scour, or of allowing the scour hole to develop. The minimum riprap size can be determined from Eq. X-3, the minimum area to be paved can be determined from Eq. X-2, and the approximate depth of the scour hole can be determined from Eq. X-4.

Eq. X-4 can be used to determine the height of the inlet invert above the bed material if no scour is to occur. This height was computed for Sand C and  $Q/D^{5/2} = 10$  to be 0.37D. Tests made both with and without the berm confirmed the prediction that no scour would take place if the inlet is located a proper distance above the erodible bed.

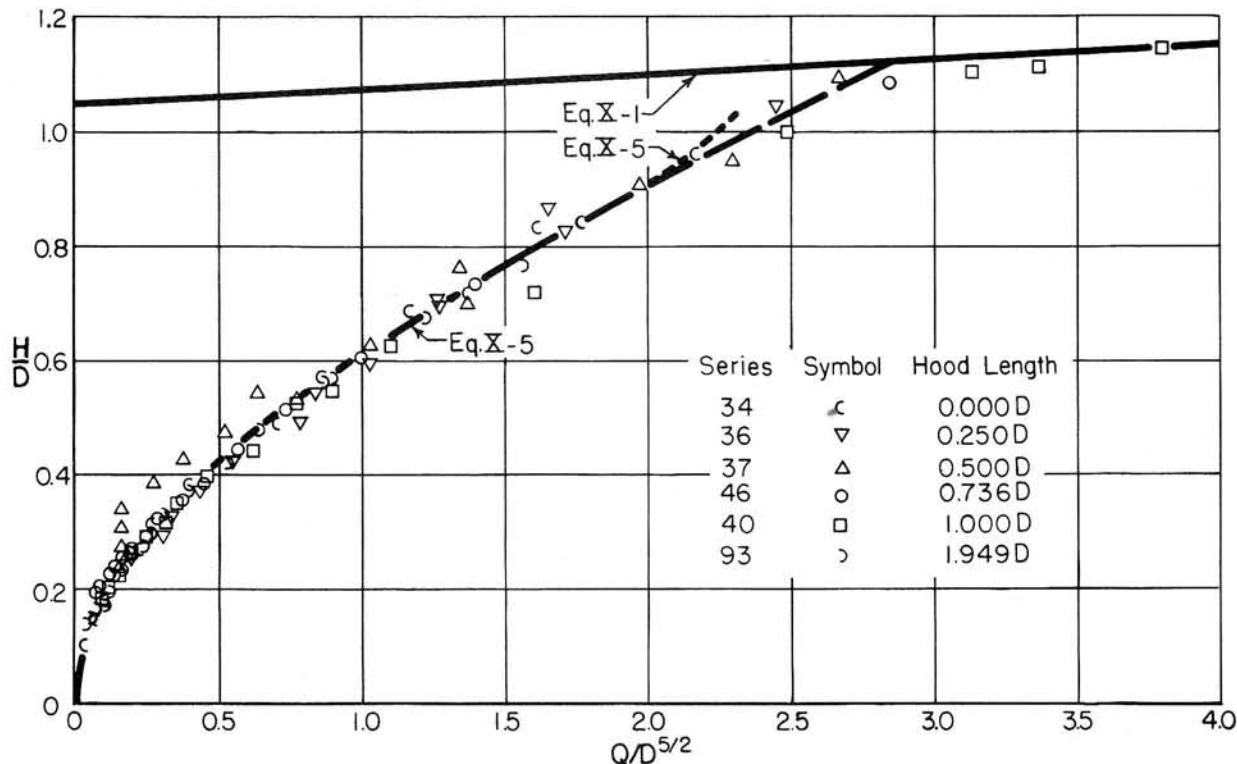


Fig. X-20 - Effect of Hood Length on Weir Flow Head-Discharge Relationship. Conduit Slope is 0.200.

The scour equations can be used to determine the minimum size of riprap required if the inlet crest is located at various distances above the surface of the riprap. If the distance below the inlet crest  $y$  and the discharge are substituted in Eq. X-4, the size of riprap that will just be picked up can be determined. Also, the depth below the crest at which the available riprap will just not be picked up can be computed by inserting  $Q$  and  $d$  in Eq. X-4.

Finally, smaller sizes of riprap can be used with increasing distance away from the inlet. These distances for various riprap sizes can be computed from Eq. X-2.

These scour tests have defined reasonably well the relationships between the bed material size, the discharge, and the scour hole dimensions for various sizes of conduit. Minimum

dimensions are given by Eqs. X-2, X-3 and X-4, and it is essential that an adequate safety factor be applied if these equations are used for design purposes.

### Spillway Capacity

At low discharges the control is the inlet acting as a weir. At high discharges the control is as for full pipe flow if the hood length is sufficient. The spillway rating curve may be determined once the weir rating curve and the entrance loss coefficient are known.

#### Capacity as a Weir

The capacity of the spillway with the entrance acting as a weir may be affected by the hood length, the conduit slope, the wall thickness, the approach conditions, or special forms of the entrance. The effect of each of these items will be discussed in turn.

**Hood Length.** The effect of hood length on the weir flow head-discharge relationship was determined for all conduit slopes. The data for all hood lengths were plotted on a single sheet for each conduit slope. Fig. X-20 is a typical plot. Some of the data for the  $D/2$  hood length in Fig. X-20 do not fit the curve well. There is no explanation for this but the water level recorder trace shows nontypical irregularities at these heads.

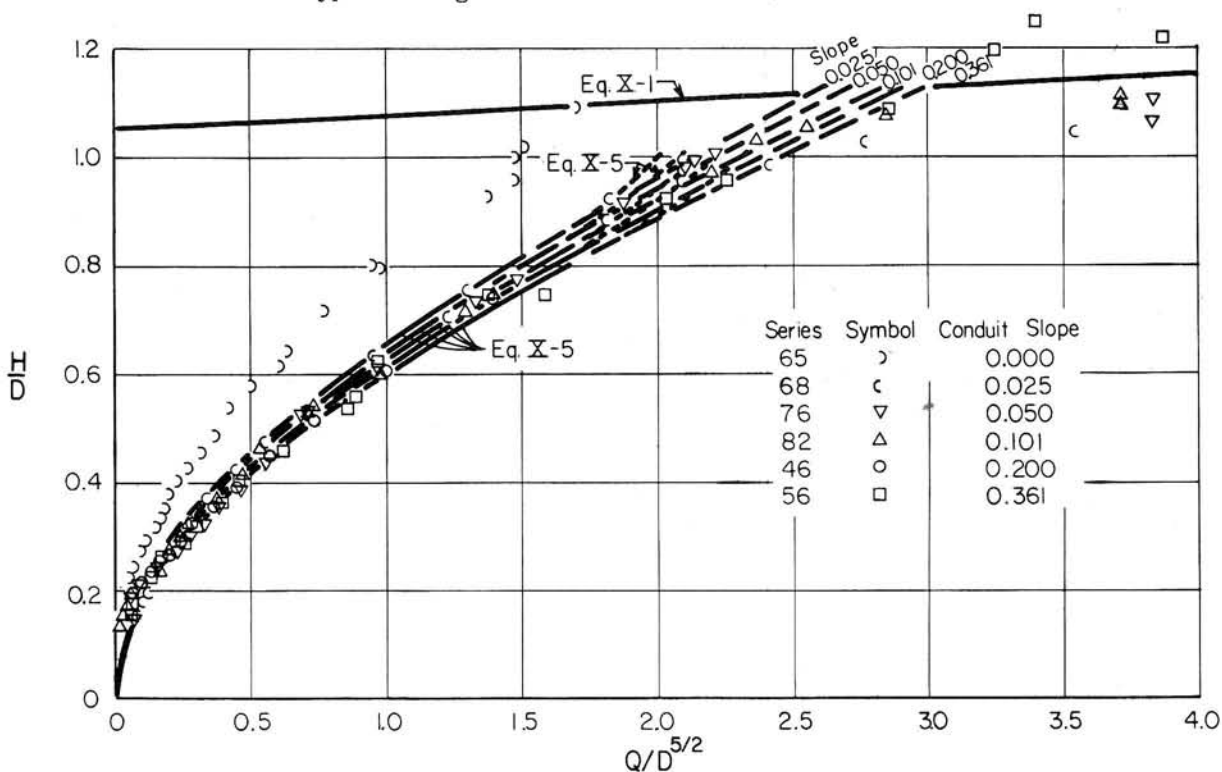


Fig. X-21 - Effect of Conduit Slope on Weir Flow Head-Discharge Relationship. Hood Length is  $3D/4$ .

There is some scatter to the data but no trend that indicates any effect of hood length on the head-discharge relationship. This is somewhat surprising in view of the wide range of hood lengths, but no other conclusion is possible. These comments apply to the data for all conduit slopes tested.

**Conduit Slope.** The conduit slope was found to have a small but significant effect on the weir flow head-discharge relationship. The data for one hood length and six conduit slopes appear in Fig. X-21. The plots for other hood lengths show similar results.

The control for the 0.025 and greater conduit slopes is at the hood inlet crest and the data plot as a family of curves. However, the control for the zero conduit slope was critical depth at the conduit exit. The head-discharge relationship at the inlet is therefore dependent on the conduit friction loss in addition to the entrance losses. It will be different for each conduit length and roughness. Although the data for the zero slope are shown in Fig. X-20, they

should not be used for design purposes. The data can be used for design purposes when the conduit slope is sufficiently steep that the control is always at the inlet.

**Conduit Wall Thickness.** Data covering the complete range of wall thicknesses tested are plotted in Fig. X-22. To avoid confusion, data for a number of intermediate wall thicknesses are not shown. No reason is known why the data at low heads for two intermediate wall thicknesses plot above the rest of the data. It possibly is one of these unexplainable things that sometimes affect experimental work. The thicknesses shown in Fig. X-22 were selected at random with no thought of picking out data that would show good agreement; data showing better agreement could have been selected. The working plots show better agreement than do the plots prepared for this paper.

The conclusion is that the wall thickness has no apparent effect on the weir flow head-discharge relationship in spite of the wide range of thicknesses tested.

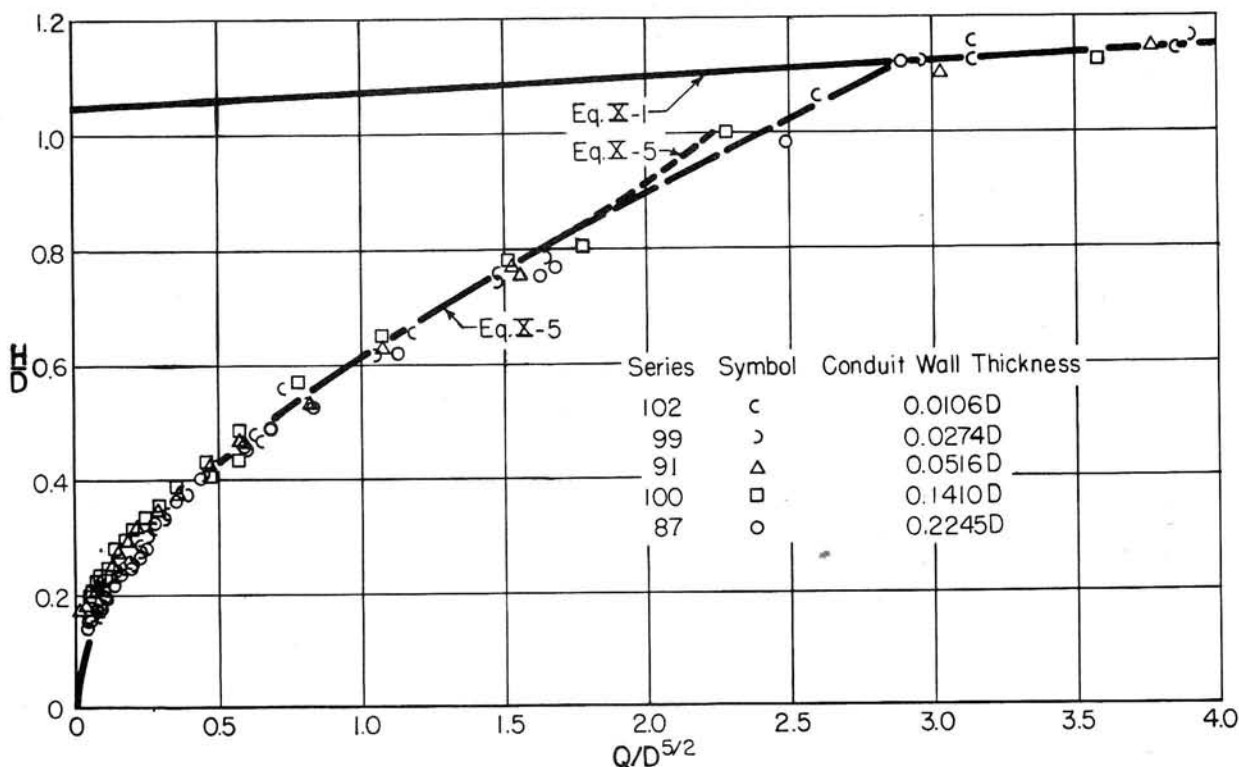


Fig. X-22 - Effect of Conduit Wall Thickness on Weir Flow Head-Discharge Relationship. Hood Length is  $3D/4$ . Conduit Slope is 0.203.

**Approach Conditions.** The number of different approach conditions tested is too limited to permit any general statements regarding their effect on weir flow. The approach conditions tested include the sloping dam face and a berm on the dam face at the crest elevation with both fixed and scoured surfaces. The data plotted in Fig. X-23 show no effect of preventing scour or of allowing the scour hole to develop. The curve shown on Fig. X-23 is the same curve shown on Figs. X-20 and X-22 and on Fig. X-21 for the 0.20 slope. Since the data plot to the right of the curve, the effect of the presence of the dam is to increase the discharge at a given head over the condition for re-entrant inlets.

**Special Inlets.** The weir flow head-discharge relationship for the sliced inlet is shown in Fig. X-24. The curve drawn is the same as is shown in Figs. X-20 to X-23 for the 0.20 slope. The head-discharge relationship is identical to that obtained for the square-edged hood inlets.

The weir flow head-discharge data for the well-rounded re-entrant inlet and the well-rounded re-entrant hood inlet are also shown in Fig. X-24. It is apparent that here again the

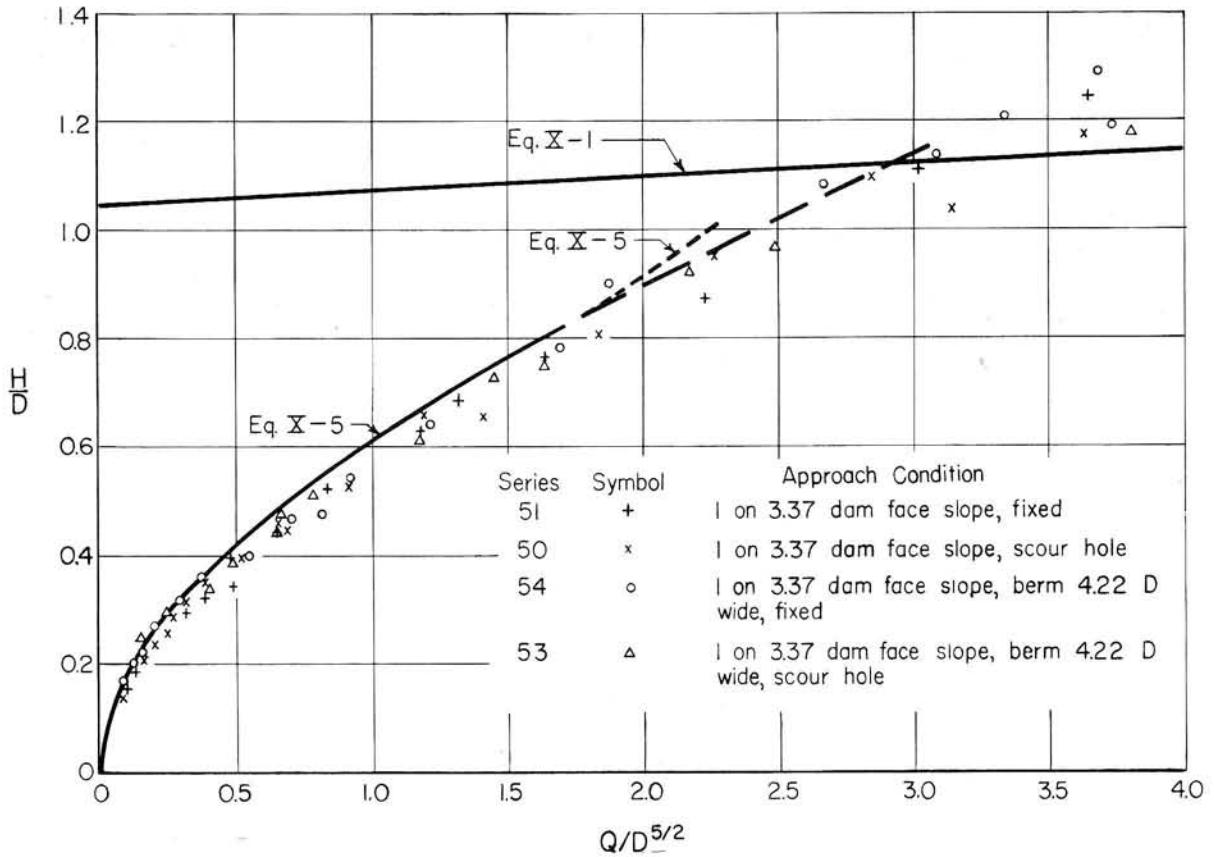


Fig. X-23 - Effect of Approach on Weir Flow Head-Discharge Relationship. Hood Length is 3D/4. Conduit Slope is 0.200.

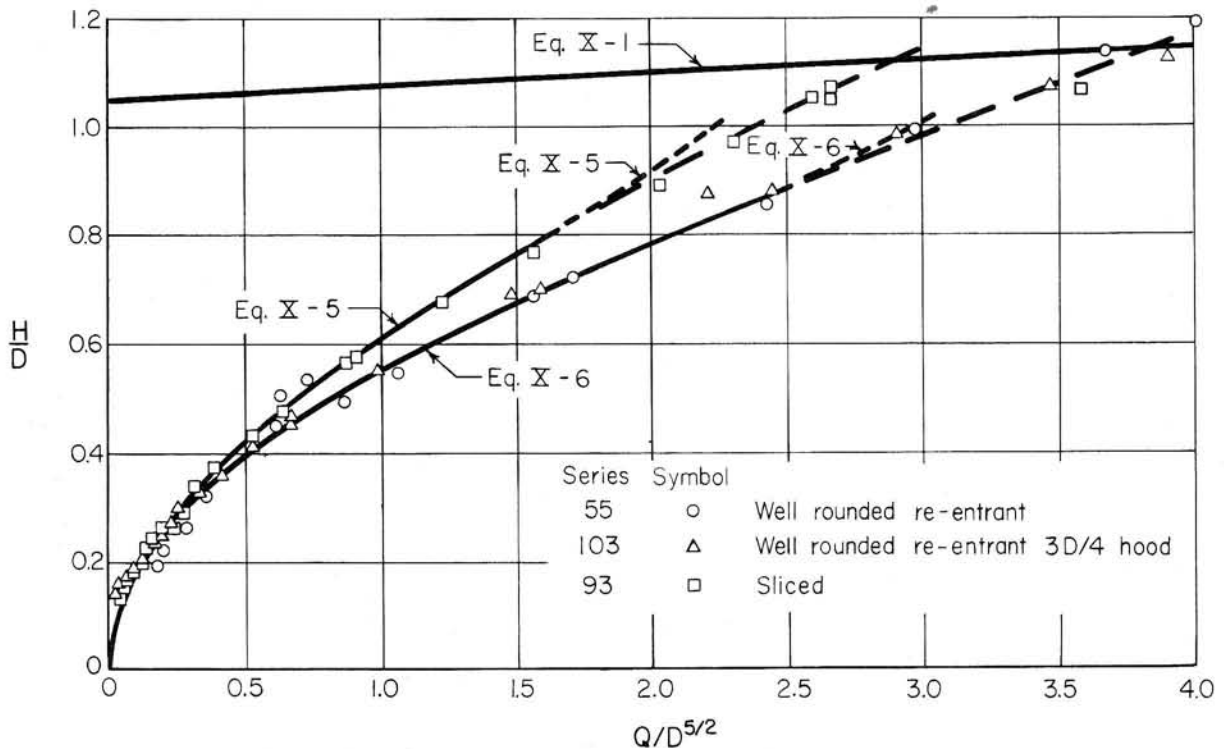


Fig. X-24 - Head-Discharge Curves for Weir Flow for Well-Rounded Re-entrant, Well-Rounded Re-entrant Hood, and Sliced Inlets.

hood has no effect on the head-discharge relationship. However, rounding results in a substantial increase in the discharge.

**Head-Discharge Equations.** The equation of the curves shown in Figs. X-20 to X-24 was developed to provide a basis for the preparation of design recommendations. The equation was developed from the theoretical equation for weir flow

$$Q = c a \sqrt{2gH}$$

where  $Q$  is the discharge in cfs,  $c$  is a dimensionless constant,  $a$  is the wetted area corresponding to a depth of flow of  $H$  in square feet,  $g$  is the acceleration of gravity in feet per sec, and  $H$  is the head in feet. The equation can be put into dimensionless terms by dividing both sides by the product of the pipe area  $A = \pi D^2/4$  and the square root of the pipe diameter  $D$ . After rearranging, this results in

$$\frac{Q}{D^{5/2}} = c \frac{\pi \sqrt{2g}}{4} \times \frac{a}{A} \sqrt{\frac{H}{D}}$$

Rearranging the terms, it is found that

$$\frac{\frac{Q}{D^{5/2}}}{\frac{a}{A} \sqrt{\frac{H}{D}}} = c \frac{\pi \sqrt{2g}}{4} = \text{constant}$$

This operation was performed on the data to evaluate the constant term. Instead of a constant,

it was found that a linear relationship existed between  $\frac{\frac{Q}{D^{5/2}}}{\frac{a}{A} \sqrt{\frac{H}{D}}}$  and  $\frac{H}{D}$ . A different

linear relationship was found for each conduit slope  $S$  when the data shown in Fig. X-21 were plotted. The effect of slope followed a logarithmic relationship. The resulting equation for the square-edged hood inlet is

$$\frac{Q}{D^{5/2}} = \left[ 1.83 S^{1/15} + 0.60 \frac{H}{D} \right] \frac{a}{A} \sqrt{\frac{H}{D}} \quad (\text{X-5})$$

This curve is shown in Figs. X-20 through X-24. The agreement with the data is seen to be excellent up to about  $0.9H/D$ . However, the equation starts to deviate from the data at about  $H/D = 0.8$  and the curves have been dotted above this head. The dashed extensions of the head-discharge curve above  $H/D = 0.8$  were drawn based on the shape of the curve given for the equation below  $H/D = 0.8$  and it can be seen that they represent the data within the obtained precision. Thus, Eq. X-5 may be used to obtain the weir flow head-discharge curve for square-edged inlets and conduits on steep slopes for heads between  $H/D = 0$  and  $H/D = 0.8$ . The curve may be extended to obtain the head-discharge relationship for the higher heads. The approximately 10 per cent increase in actual discharge shown in Fig. X-23 obtained when a dam is used over that given by the equation should be considered a safety factor. The present data are too few to justify general recommendations of increased flow for certain approach conditions.

Weir flow is not the control for heads in excess of those given by Eq. X-1. The curve of Eq. X-1 is shown in Figs. X-20 through X-24 to define this upper limit of weir control.

The greater discharge obtained with the well-rounded inlets is given by the equation

$$\frac{Q}{D^{5/2}} = \left[ 1.83 S^{1/15} + 1.35 \frac{H}{D} \right] \frac{a}{A} \sqrt{\frac{H}{D}} \quad (\text{X-6})$$

The agreement of this curve with the data is shown in Fig. X-24. The well-rounded inlets were tested on only one slope but the data fit the slope data obtained for the square-edged inlet. The slope correction in Eq. X-6 is therefore based on the square-edged inlet data.

TABLE X-5

VALUES OF  $\frac{a}{A} \sqrt{\frac{H}{D}}$

$\frac{H}{D}$	.00	.01	.02	.03	.04	.05	.06	.07	.08	.09
0.0	.0000	.0002	.0007	.0015	.0027	.0042	.0060	.0081	.0106	.0134
0.1	.0164	.0199	.0236	.0275	.0318	.0364	.0413	.0465	.0519	.0577
0.2	.0637	.0700	.0765	.0833	.0904	.0978	.1053	.1132	.1213	.1296
0.3	.1382	.1470	.1561	.1653	.1748	.1845	.1945	.2046	.2149	.2255
0.4	.2362	.2472	.2583	.2696	.2811	.2928	.3046	.3166	.3287	.3411
0.5	.3536	.3661	.3789	.3918	.4048	.4179	.4312	.4445	.4580	.4716
0.6	.4853	.4990	.5128	.5267	.5407	.5547	.5688	.5829	.5971	.6114
0.7	.6256	.6398	.6540	.6683	.6825	.6967	.7110	.7251	.7392	.7531
0.8	.7670	.7809	.7947	.8083	.8218	.8352	.8485	.8614	.8742	.8869
0.9	.8994	.9115	.9232	.9347	.9457	.9565	.9667	.9763	.9852	.9933
1.0	1.0000									

Values of  $a/A$  for various values of  $H/D$  may be taken from King [I-31 Table 98, page

295]. However, to facilitate the use of Eqs. X-5 and X-6, values of  $\frac{a}{D} \sqrt{\frac{H}{D}}$  have been computed. They are listed in Table X-5.

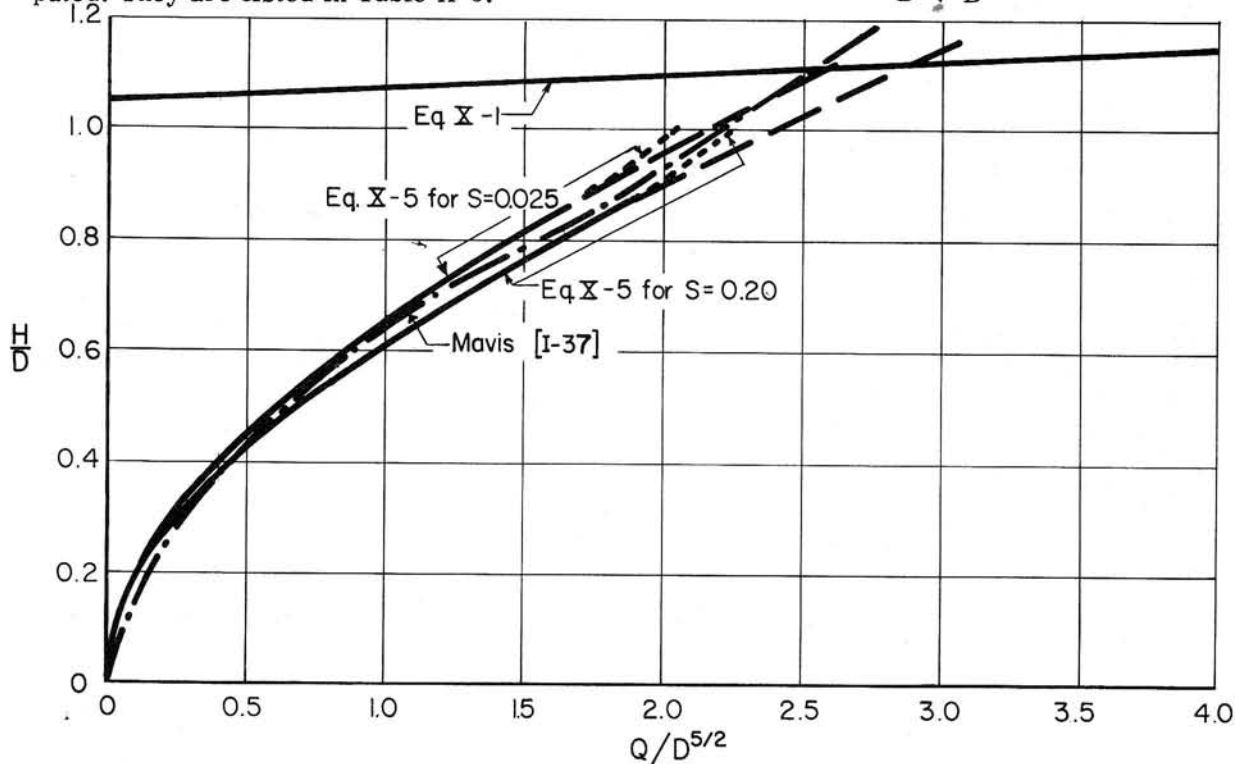


Fig. X-25 - Comparison of Hood Inlet Weir Flow Head-Discharge Equations with Mavis' Curve.

**Comparison with Mavis' Curve.** The work of Mavis [I-37] on culvert hydraulics has been widely used and often quoted. A comparison of Eq. X-5 with the weir flow head-discharge curve presented by Mavis [I-37, Fig. 23] for square-edge entrances is therefore of interest. The principal difference between the inlets is that Mavis used a plane headwall while here the inlets were re-entrant. Also, Mavis' range of slopes was only from 0.007 to 0.0657 and he has indicated no effect of slope. The comparison is made in Fig. X-25. It is interesting to note that the agreement is generally good.

### Entrance Loss for Full Conduit Flow

The entrance loss coefficient for full flow is affected considerably by the hood angle, the conduit wall thickness, the shape of the entering edge, and the approach conditions. The conduit slope has no effect, and the effect of the various anti-vortex walls is not large.

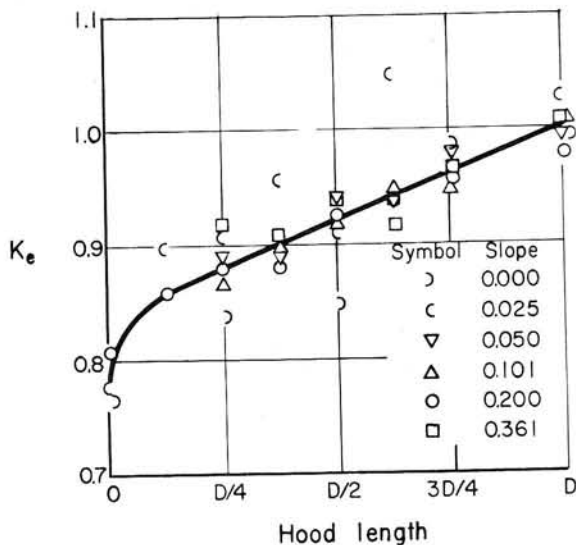


Fig. X-26 - Effect of Hood Length on Entrance Loss Coefficient. Square-Edged Inlet.  $t_p/D = 0.015$ .

ratio of the pipe wall thickness  $t_p$  to the pipe diameter  $D$  is greater than about 0.04. The loss coefficient is variable and the wall is classified as thin when  $t_p/D$  is less than 0.04. This is shown in Fig. X-27. The data plotted in Fig. X-27 includes data on walls as thin as it was possible to test. Thinner walled inlets were built but they broke under test before data could be obtained.

The three low data points were obtained early in the test program. The reason why they are low cannot be explained. The same inlets were tested again with the results shown by points plotted directly above the low points.

The theoretical and experimental curves obtained by Harris [I-24] are shown in Fig. X-27, because they show the same shape as the curve obtained for the hood inlet. The wall thickness obtained by Harris at which the coefficient ceases to vary with wall thickness is seen to be the same as that obtained for the hood inlet.

The test results show, for the square-edged hood inlet having a hood length of  $3D/4$ , that

$$K_e = 1.08 - 0.6 \frac{t_p}{D} \quad \text{for} \quad \frac{t_p}{D} < 0.04 \quad (\text{X-7a})$$

(thin-walled inlets), and that

**Conduit Slope.** The average entrance loss coefficient  $K_e$  for each series shows no trend when plotted against the conduit slope  $S$ . The inlets were re-entrant and the water had free access to all sides of the inlet for all conduit slopes. Therefore, the finding that conduit slope has no effect on the entrance loss is entirely reasonable.

**Hood Length.** The effect of the hood length on the entrance loss coefficient is definite and considerable. The results of the tests are shown in Fig. X-26. This significant effect for full flow contrasts with the lack of any such effect for weir flow shown in Fig. X-20. Fig. X-26 demonstrates that there is a small but definite hydraulic advantage in using the shortest hood length that will insure satisfactory hydraulic performance.

**Conduit Wall Thickness.** The walls of the hood inlet may be classed as thin or thick. The entrance loss coefficient  $K_e$  is constant and the wall is classified as thick when the

TABLE X-6  
EFFECT OF ANTI-VORTEX DEVICE ON ENTRANCE LOSS COEFFICIENT AND PRESSURE

Series	Anti-Vortex Device	$K_e$	$h_r/h_{vp}$	
			Crown <sup>a</sup>	Invert <sup>b</sup>
39	Fig. 12a	0.96	--	-0.64
46	Fig. 12b	0.95	+0.72	-0.55
47	Fig. 12c	0.98	+0.72	-0.58
48	Fig. 12d	1.01	+0.22	-0.60
49	Fig. 12e	0.85	+0.67	-0.50
106	Fig. 12f	0.83	+0.52	-0.79

<sup>a</sup>At crown OD inside conduit.

<sup>b</sup>At invert 0.5D inside conduit.

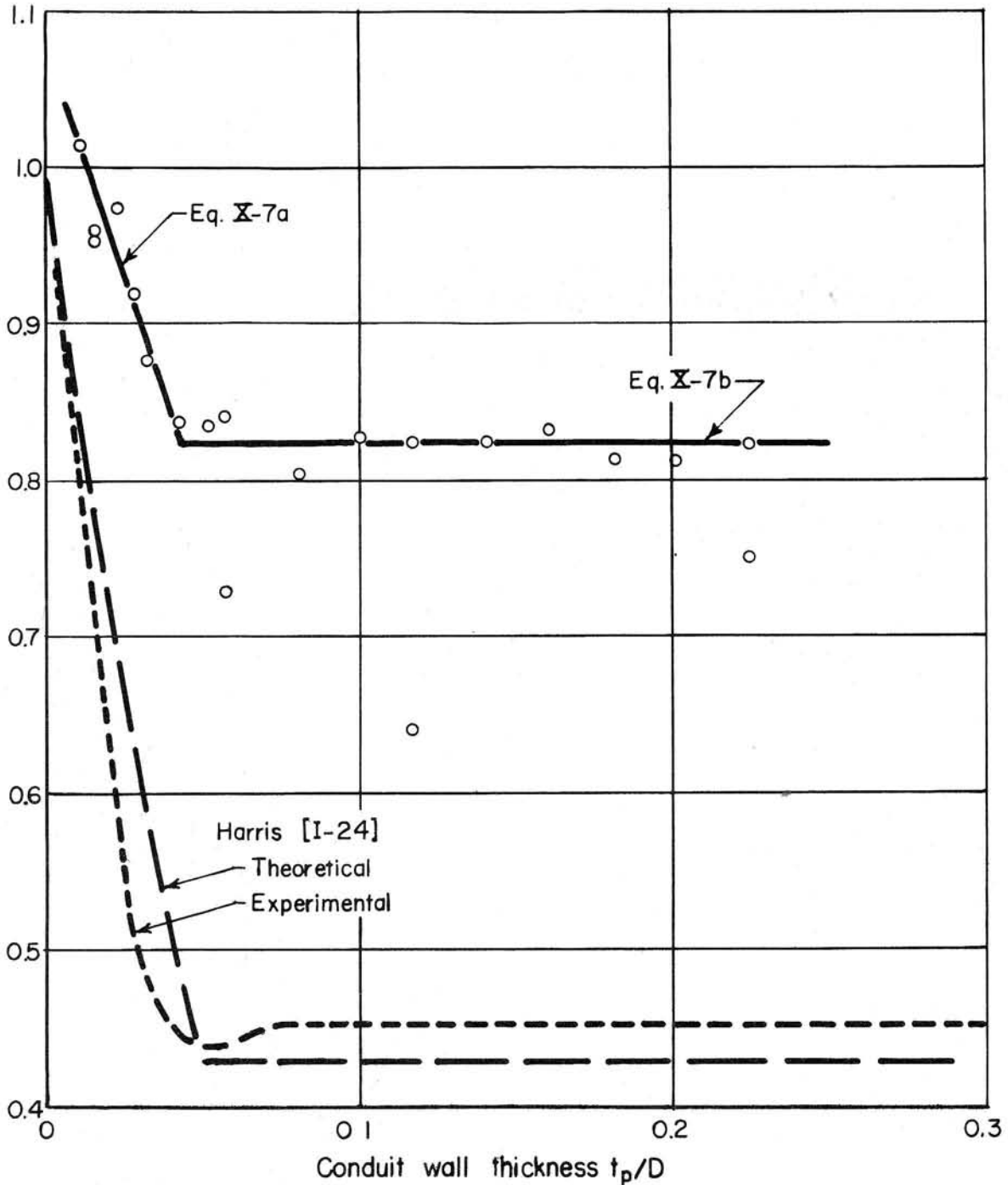


Fig. X-27 - Effect of Conduit Wall Thickness on Entrance Loss Coefficient. Square-Edged Inlet. Hood Length is  $3D/4$ . Conduit Slope is 0.20.

$$K_e = 0.825 \quad \text{for} \quad \frac{t_p}{D} > 0.04 \quad (\text{X-7b})$$

(thick-walled inlets).

**Anti-Vortex Device.** The various types of anti-vortex devices that were tested are shown in Fig. X-12. Their effect on the entrance loss coefficient is shown in Table X-6.



TABLE X-7  
EFFECT OF APPROACH ON ENTRANCE LOSS COEFFICIENT AND PRESSURE  
Hood Length =  $3D/4$  Conduit Slope = 0.20  $t/D = 0.0156$

Series	Approach Condition	$K_e$	$h_n/h_{vp}$	
			Crown <sup>a</sup>	Invert <sup>b</sup>
51	1 on 3.37 dam face slope, fixed	0.80	+0.57	-0.31
50	1 on 3.37 dam face slope, scour hole	0.93	+0.71	-0.50
54	1 on 3.37 dam face slope, berm $4.22D$ wide, fixed	0.84	+0.38	-0.21
53	1 on 3.37 dam face slope, berm $4.22D$ wide, scour hole	0.93	+0.66	-0.43
46	re-entrant	0.95	+0.72	-0.55

<sup>a</sup>At crown OD inside conduit. <sup>b</sup>At invert 0.5D inside conduit.

There is no difference between the two splitter type anti-vortex walls shown in Fig. X-12a and X-12b. They are so alike that no difference should be expected. Extending the anti-vortex wall down in front of the inlet and bringing it closer to the inlet, as in Figs. X-12c and X-12d, causes a small increase in the entrance loss coefficient. The headwall type anti-vortex wall shown in Fig. X-12e apparently suppresses the contraction at the inlet and causes a considerable decrease in the entrance loss coefficient. However, the efficiency of this wall in vortex control is somewhat less than the splitter walls. The entrance loss coefficient for the anti-vortex plate shown in Fig. X-12f is the lowest obtained. This, then, is the best anti-vortex device considering both its low loss coefficient and its vortex inhibiting ability.

Approach Conditions. The use of a paved approach to the hood inlet results in a significant reduction in the entrance losses. This is shown in Table X-7. The entrance loss coefficient is lowest if no berm is used.

The entrance loss is almost equal to that for the re-entrance inlet if the approach to the hood inlet is not paved and a scour hole is allowed to develop.

Such data as is presently available on different approach conditions shows that a significant reduction in the entrance loss is possible if the approach is paved to prevent scour of the dam in the vicinity of the inlet.

Special Inlets. The entrance loss coefficients for the special inlets are listed in Table X-8. Also listed in Table X-8 are comparative coefficients for the square-edged hood inlets. The least entrance loss is obtained for the inlet having a  $0.21D$  radius rounding and no hood. The next best inlet is a  $3D/4$  hood inlet with a radius of rounding of  $0.21D$  at the entrance. These coefficients are 0.10 and 0.16, respectively, and are quite low. They show, as do the data for the square-edged inlet presented in Fig. X-26, an increased entrance loss when the hood is used. In contrast, a hood is not needed for satisfactory performance if the inlet is well-rounded while a hood inlet is required for satisfactory performance if the inlet is square-edged.

The entrance loss for the sliced inlet was the highest observed.

TABLE X-8  
ENTRANCE LOSS COEFFICIENTS AND PRESSURES FOR SPECIAL INLETS  
Conduit Slope = 0.20

Series	Inlet	$K_e$	$h_n/h_{vp}$	
			Crown <sup>a</sup>	Invert <sup>b</sup>
55	Well-rounded, re-entrant	0.10	-0.21 <sup>a</sup>	-0.32 <sup>b</sup>
103	Well-rounded, re-entrant, $3D/4$ hood	0.16	+0.16 <sup>c</sup>	-0.21 <sup>d</sup>
93	Sliced	1.29	+0.96 <sup>e</sup>	-0.30 <sup>b</sup>
Ave.	Square-edged, re-entrant, thick-walled, $3D/4$ hood	0.825	+0.50 <sup>e</sup>	-0.8 <sup>b</sup>
104	Square-edged, re-entrant, thin-walled ( $t/D = 0.0116$ ), $3D/4$ hood	1.02	+0.70 <sup>e</sup>	-0.54 <sup>b</sup>

<sup>a</sup>At crown 0.25D inside conduit. <sup>b</sup>At invert 0.5D inside conduit. <sup>c</sup>At crown 0.03D inside conduit.  
<sup>d</sup>At invert 0.67D inside conduit. <sup>e</sup>At crown OD inside conduit.

The results presented here show that the well-rounded inlets give the lowest entrance loss.

Capacity as an Orifice

An orifice at the entrance controls the head-discharge relationship only for the short hood lengths; orifice control does not exist for the longer hood lengths. The use of short hood lengths is not recommended since it is possible to have both orifice and pipe control at the same head. This is shown in Fig. X-28 for a number of hood lengths and for two conduit slopes. The weir flow data are not plotted in Fig. X-28 because it has been shown in Fig. X-20 that the

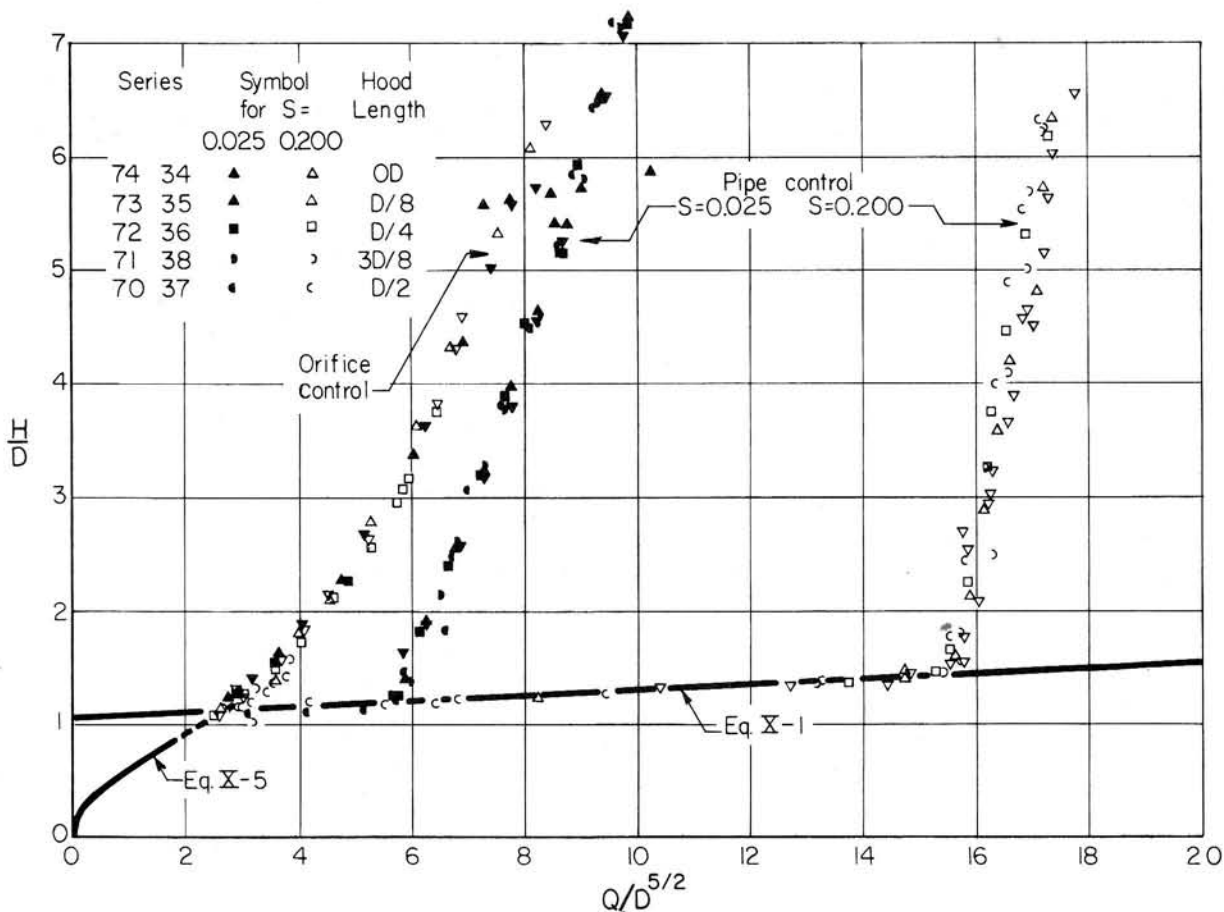


Fig. X-28 - Head-Discharge Curves for Short Hood Lengths Where the Entrance Orifice May Control.

same curve is obtained for all hood lengths. In spite of the fact that the hood lengths that produce orifice control are not recommended, the data obtained on orifice coefficients will be presented to place it on record. It can be seen in Fig. X-28 that the orifice head-discharge curve is the same for the two conduit slopes for which comparable data are available.

The coefficient of discharge  $C_o$  for orifice control is given by the equation

$$Q = C_o A_o \sqrt{H_o} \tag{I-7}$$

In Eq. I-7 the orifice area  $A_o$  is taken at the plane of the entrance; it is equal to the conduit area divided by the cosine of the hood angle. The head  $H_o$  is measured from the center of the orifice.

The orifice coefficient of discharge is presented in Fig. X-29 for all runs in which orifice control was obtained. Orifice control existed at all heads for the OD and D/8 hood

lengths. For the  $D/4$  hood length, orifice control existed only to  $H_o/D$  values of 3.25 and then the conduit filled. The corresponding figure for the  $3D/8$  hood length is 1.35. Orifice control data were not obtained for all slopes when the hood length was  $D/2$  and such data as were obtained extended only to  $H_o/D = 0.9$ .

There is some scatter to the data presented in Fig. X-29. However, the trend of the data shows that  $C_o$  increases rapidly between  $H_o/D$  values of 0.5 and 1, reaches a maximum when  $H_o/D$  approximates 2, and then drops to what appears to be a constant value of about 4.4 when  $H_o/D$  exceeds about 4. These orifices were square-edged, re-entrant, and had wall thicknesses  $t_p/D$  of 0.015.

### Pressures

The pressure within the conduit--the hydraulic grade line pressure--coincides with the friction grade line throughout most of the conduit length. However, the inlet causes local deviations near the conduit entrance. These pressures are of concern if they result in absolute pressures close to or below the vapor pressure. The local pressure deviation from the friction grade line  $h_n$  has been computed as a ratio to the velocity head in the conduit  $h_{vp}$  assuming that the hydraulic grade line passes through the center of the conduit exit. This assumption is somewhat in error, as will be pointed out later. The error varies with the conduit slope, the least error occurring for the 0.050 slope. While the data presented in Fig. X-30 show an effect of slope for the short hood lengths, the effect of slope on the pressures is hidden in the experimental variations for the longer hood lengths, Fig. X-30 shows that the pressures increase with the hood length, that the crown pressure  $0.5D$  inside the entrance is generally  $0.7 h_{vp}$  greater than the invert pressure at the same station along the conduit, and that the crown pressure directly over the invert at the conduit entrance is positive and somewhat greater than the crown pressure  $0.5D$  further downstream.

The effect of conduit wall thickness on the pressure is shown in Fig. X-31. The data has the same trend as the entrance loss coefficient data shown in Fig. X-27. The minimum pressure, which is important in evaluating the possibility of cavitation, is  $-0.8 h_{vp}$ . This pressure is almost constant for all wall thicknesses in excess of  $0.04D$  and is higher for the thinner walled conduits.

The effect of the anti-vortex wall on the pressure is given in Table X-6. The crown pressure is reduced by the Fig. X-12d anti-vortex wall but it is still safely positive. The head-wall type anti-vortex wall (Fig. X-12e) seems to increase the pressure at the invert while the crown pressure is about the same as for the splitter type anti-vortex walls. The anti-vortex plate reduces both the invert and the crown pressures.

The approach conditions affect the pressures with the paved berm producing the least disturbance to the flow, i.e.,  $h_n/h_{vp} = 0$ , as is shown in Table X-7. The presence of a scour hole permits greater flow disturbance.

The pressures for the special inlet are given in Table X-8. Abnormal pressures are shown even for the well-rounded inlets even though the abnormality is not great.

The data indicate that the minimum pressure at the square-edged re-entrant entrance will be  $0.8 h_{vp}$  below the friction grade line when the hood length is  $3D/4$ . If a scour hole is allowed to form in the dam fill, the minimum pressure may be raised to  $-0.5 h_{vp}$  while if the approach is paved the minimum pressure can be further raised to  $-0.3 h_{vp}$  or  $-0.2 h_{vp}$  without and with a berm respectively. The minimum pressure for a re-entrant well-rounded inlet is about  $-0.3 h_{vp}$ .

### Hydraulic Grade Line

The hydraulic grade line for the full conduit did not pierce the conduit at its centerline when it was extended to the plane of the conduit exit. The elevation of the hydraulic grade line at the exit was determined by plotting the grade line from piezometric measurements made along the conduit and extending it to the conduit exit. The elevation of this line above the elevation of the conduit invert at the exit divided by the conduit diameter is designated  $\beta$  and is

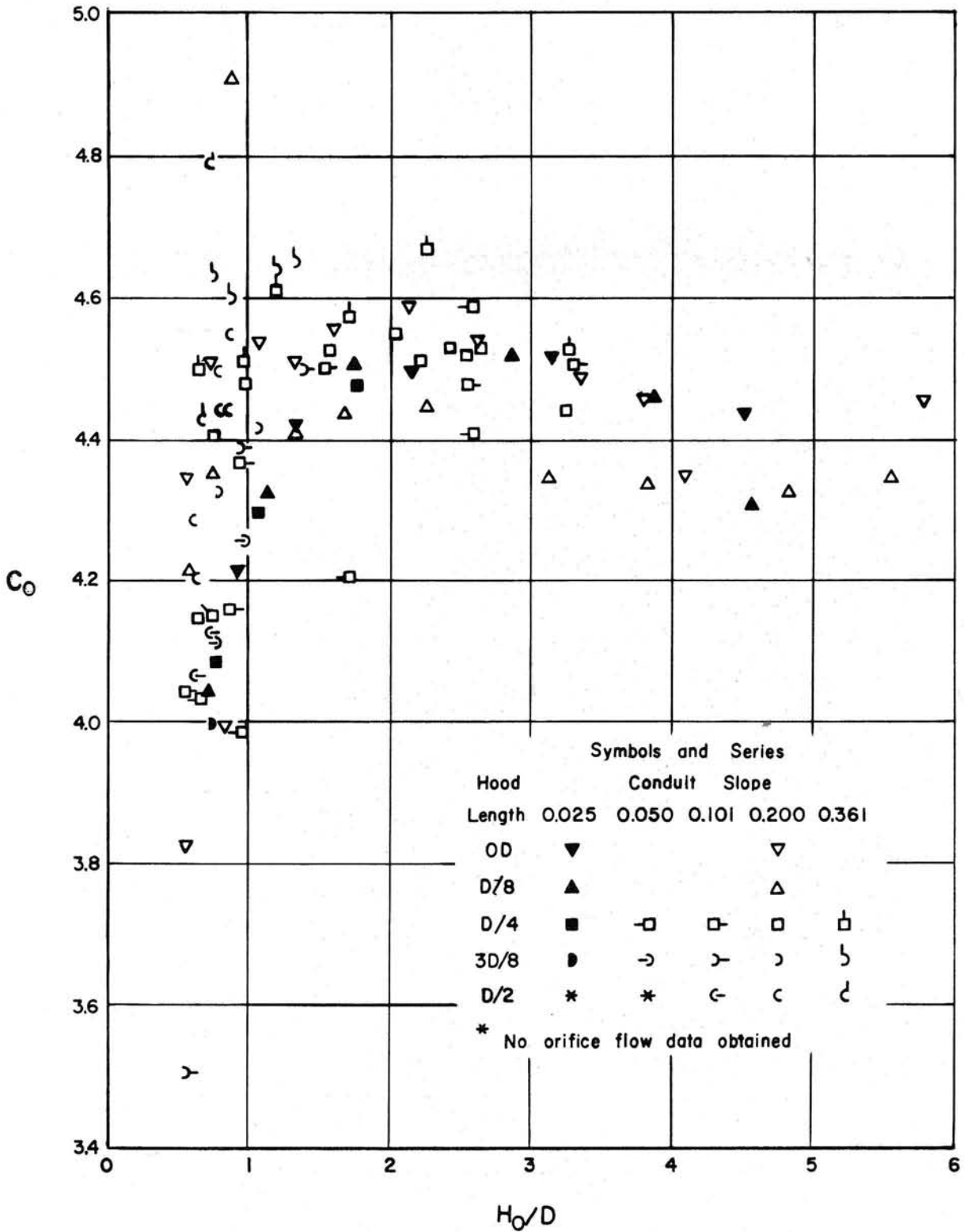


Fig. X-29 - Discharge Coefficient for Orifice Control.

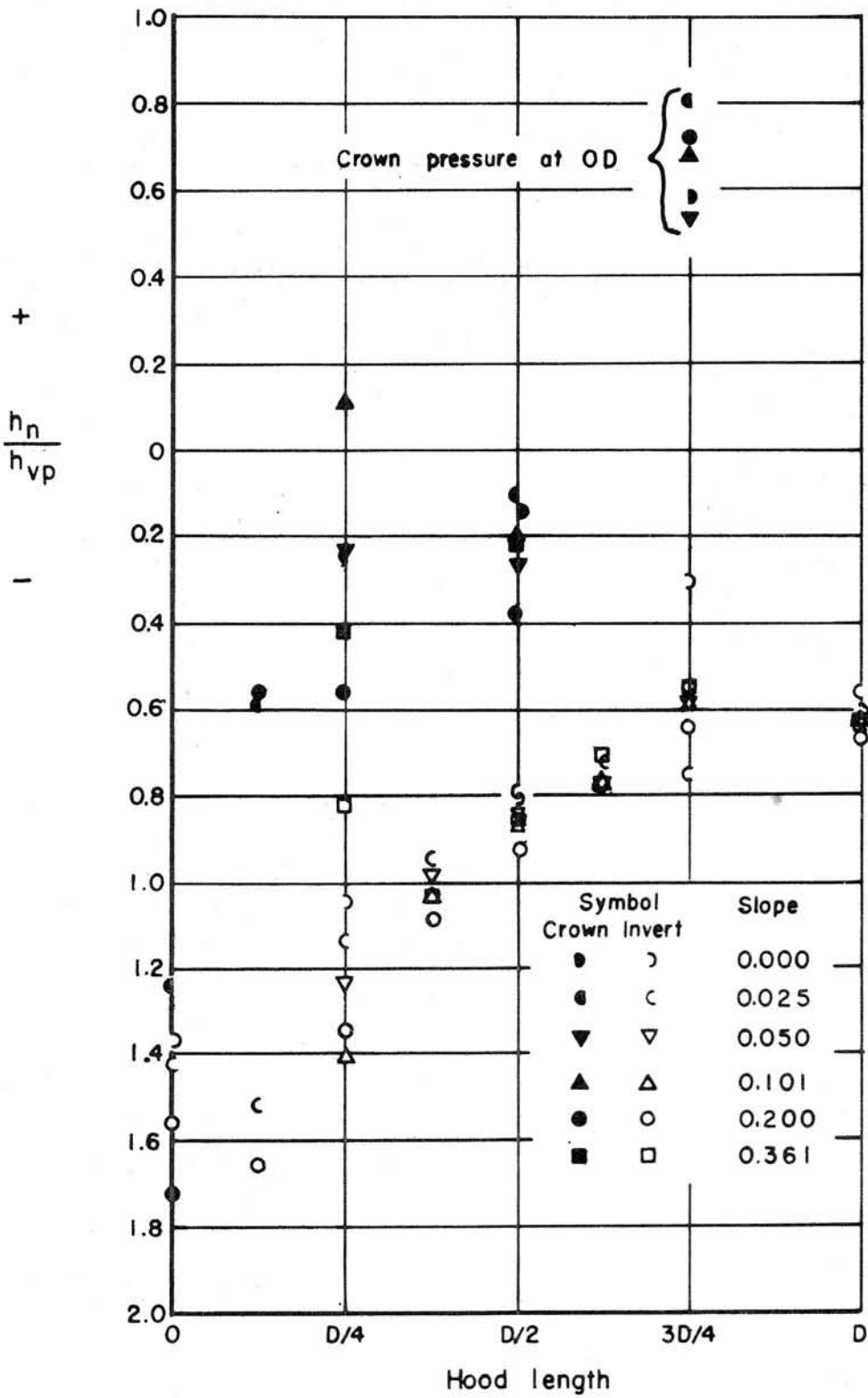


Fig. X-30 - Influence of Hood Length on Pressure in Conduit 0.5D Downstream from the Entrance. Square-Edged Re-entrant Entrance.  $t_p/D = 0.015$ .

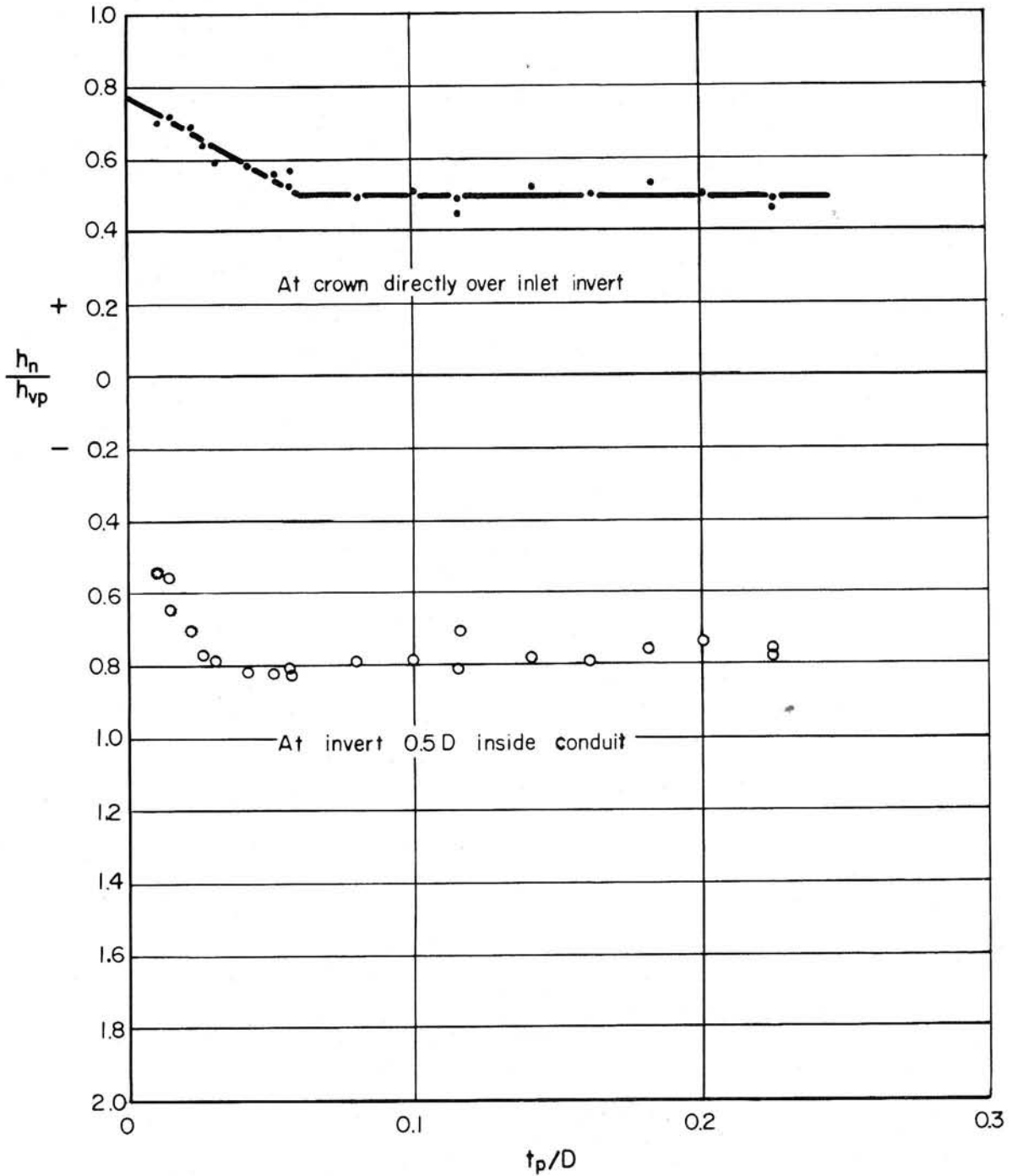


Fig. X-31 - Effect of Wall Thickness on Pressure. Square-Edged Re-entrant Inlet. Hood Length is  $3D/4$ . Conduit Slope is 0.20.

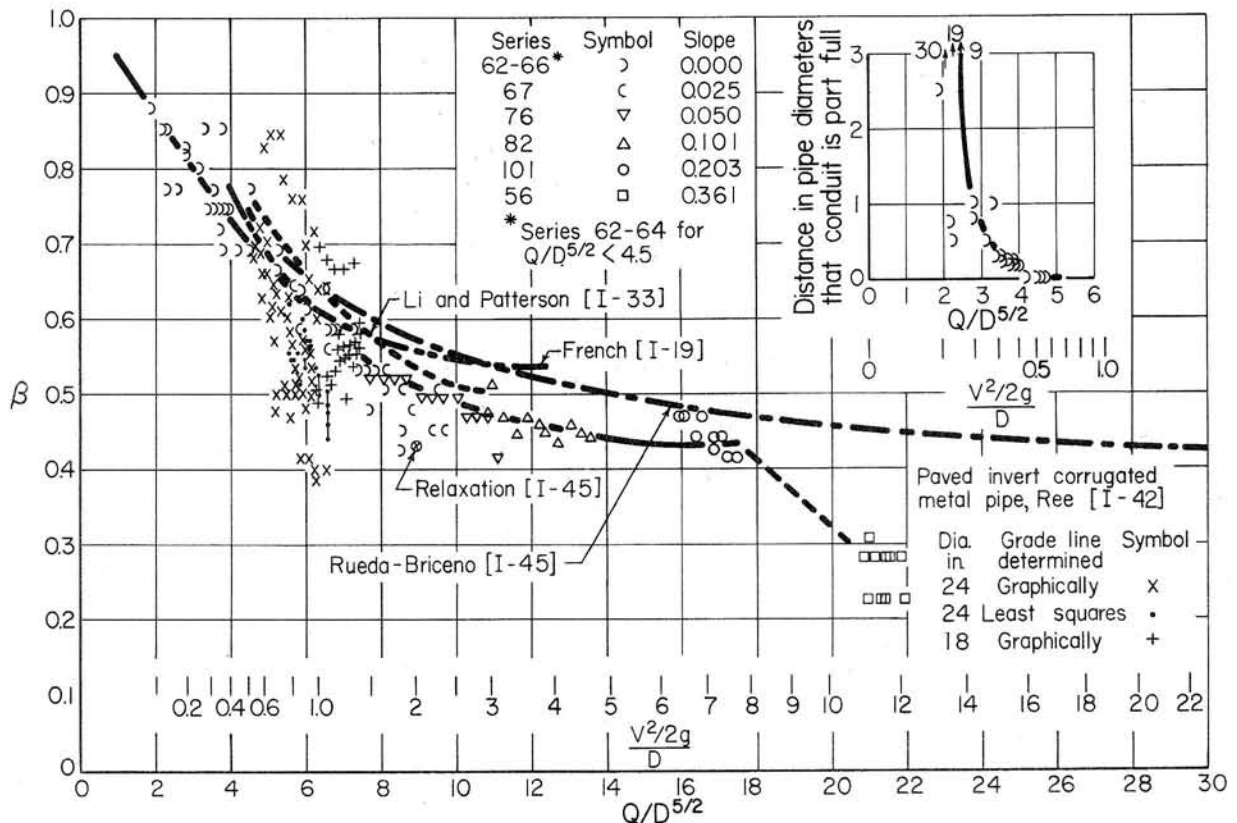


Fig. X-32 - Position of the Hydraulic Grade Line at the Conduit Exit.

plotted in Fig. X-32. Not all of the available data have been plotted; to do so would result in an indistinguishable mass. The data presented well represent the data not plotted.

The position of the hydraulic grade line at a freely-discharging conduit exit is seen in Fig. X-32 to be a function of the relative discharge  $Q/D^{5/2}$  or of the velocity head divided by the pipe diameter  $\frac{V^2/2g}{D}$ . The curve defined by the data is quite regular except for the

steepest conduit slope. No firm explanation for this deviation is available, although the waste receiver may have caused a reduction in the pressure at the conduit exit.

The data obtained by Ree [I-42] for 24-in. and 18-in. paved invert corrugated metal pipe, supplemented by a letter from Mr. Ree, is also plotted. Mr. Ree determined some of the hydraulic grade lines by least squares, but since the results closely approximated those obtained graphically, he used the easier graphical method for most determinations. There is some scatter to Ree's data and the points generally fall below the curve. However, there are enough points above the curve to indicate that the curve may fairly well represent the grade line position at the conduit exit.

The curves obtained by French [I-19], Li and Patterson [I-33], and Rueda-Briceño [I-45] are shown for purposes of comparison. Also shown is a single point computed for a two-dimensional conduit by McNown and Sarpkaya using the relaxation method [I-45].

The conduit was not full for its entire length for some of the lower discharges. The length of the conduit near the exit which was only partly full is shown in the upper right hand corner of Fig. X-32. The hydraulic grade line for these data was determined in the portion of the conduit which was completely full and was projected to the plane of the outlet as was done for the completely full conduit.

The position of the hydraulic grade line at the exit of a conduit flowing full and discharging freely is shown in Fig. X-32 to depend upon the discharge. It is apparent that a definite answer has not yet been obtained and that further study is highly desirable.

## CONCLUSIONS AND RECOMMENDATIONS

Only the desirable weir and pipe controls exist for the hood inlet if the hood length is  $3D/4$ . The undesirable orifice control may exist for short hood lengths. The shortest hood which will insure full conduit flow at minimum headwater elevation is  $3D/4$ .

There is no influence of conduit slope on the spillway performance if the slope is steep.

A vortex inhibitor of some type is a necessity. The anti-vortex devices shown in Fig. X-12 are recommended. However, the device shown in Fig. X-12e is the least satisfactory.

The capacity of the spillway acting as a weir is given by Eqs. X-5 and X-6; the capacity for flow of a mixture of air and water is given by Eq. X-1; and the entrance loss coefficient for full pipe flow and square-edged entrances is given by Eqs. X-7. Entrance loss coefficients for special inlets are presented in the paper.

The thickness of the conduit wall did not affect the hood inlet performance or its capacity as a weir. The effect of thickness on the entrance loss coefficient is given by Eqs. X-7.

Although there was little variation in approach conditions, the approach had no influence on the spillway performance. The presence of the dam face does somewhat reduce the entrance loss coefficient.

High velocities near the hood inlet may erode the dam. The size of the scour hole is small and it may prove desirable to allow it to form rather than to prevent scour. The scour hole dimensions are given by Eqs. X-2 and X-4. The size of stone which is in imminent danger of being picked up is given by Eq. X-3. Eq. X-3 also gives the size of riprap required for various flows, Eq. X-2 gives the radius of the area requiring protection, and Eq. X-4 gives the height of the hood inlet above the erodible material if scour is to be prevented. It is stressed that Eqs. X-2, X-3 and X-4 give minimum dimensions. An ample safety factor should be applied.

Pressures within the hood inlet are a maximum of  $0.8 h_{vp}$  below the hydraulic grade line. The pressures for thin wall inlets are a little higher and reference should be made to Fig. X-30 if it is necessary to refine the pressure computations.

The position of the hydraulic grade line at the conduit exit varies with the discharge. More information is needed to define adequately its position.

## ACKNOWLEDGEMENTS

The study of hood inlets was performed by the Soil and Water Conservation Research Division, Agricultural Research Service, U.S. Department of Agriculture in cooperation with the Minnesota Agricultural Experiment Station and the St. Anthony Falls Hydraulic Laboratory under the direction of William C. Ackermann, former Head, and Austin W. Zingg, Chief, Watershed Technology Research Branch. The authors performed the experiments and made the analyses with the help of Robert Dart and Harold Krueger.